Compensation of Loudspeaker Driver Nonlinearities Using Predictive And Feed Back-Based Approaches

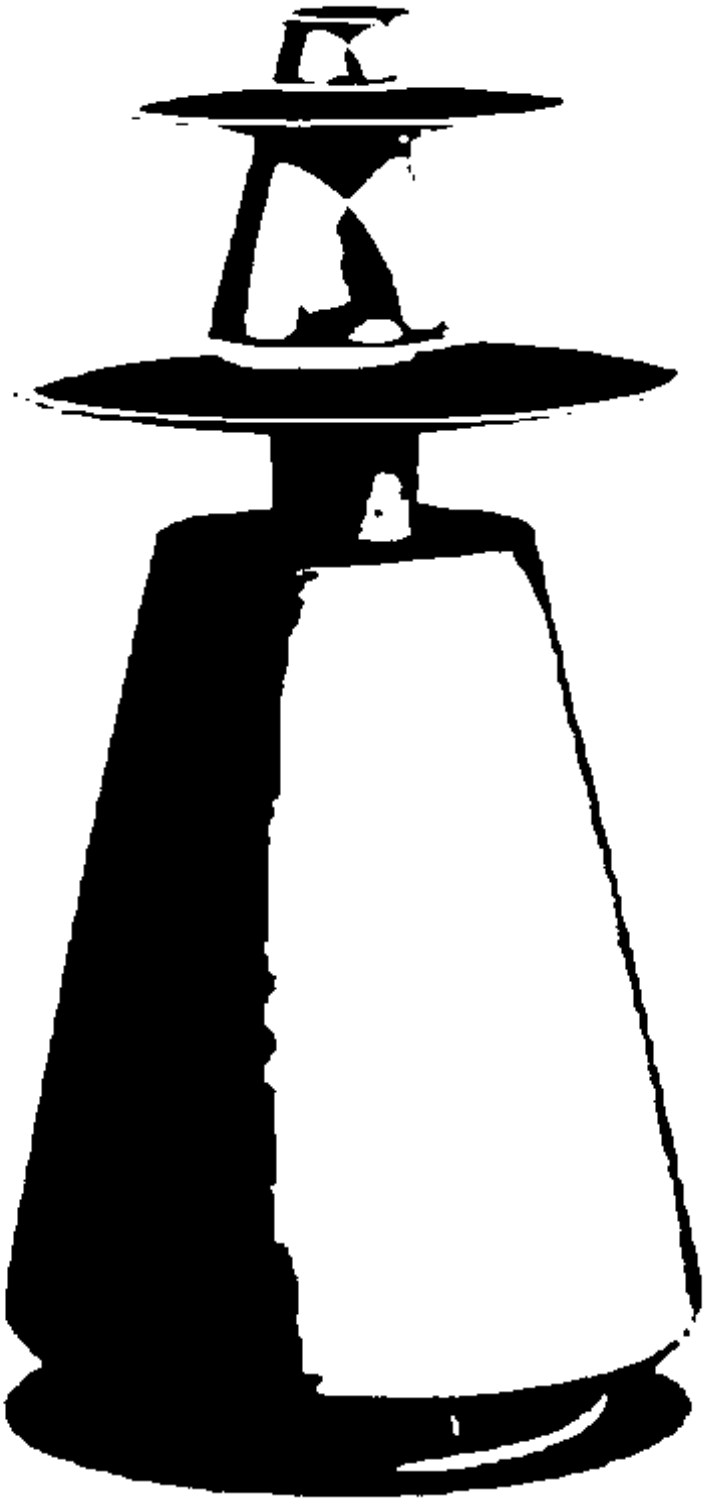

Heine Falkesgaard & Michael Hundsdahl
Department of Electronic Systems
Automation and Control Section
Aalborg University
Master Thesis
2008

AALBORG UNIVERSITY

Department of Electronic Systems
Fredrik Bajers Vej 7C
Telefon 96 35 87 00
Fax 98 15 17 39
http://www.control.aau.dk

Title:
Compensation of Loudspeaker Driver Nonlinearities Using Predictive and Feedback-Based Approaches

Project period:
September 2007 - June 2008

Group:
1035

Members:
Heine Falkesgaard
Michael Hundsdahl

Supervisor:
Jakob Stoustrup

Copies: 5

Pages: 85

Appendices: 4

Concluded: 4th of June 2008

Synopsis:

This thesis treats the problem with nonlinearities in a loudspeaker driver. The hypothesis was: Can the harmonic distortion in a loudspeaker driver be removed using control knowledge? The loudspeaker driver was studied and a mathematical model of a driver was made. The mathematical model was analysed and reduced. To remove the harmonic distortion this thesis analysed the model, and located the nonlinear elements producing the harmonic distortion. A control scheme was presented and designed.
The scheme consisted of a controller, a closed loop observer and a adaptive estimator. The controller designed, uses the nonlinear control type feedback linearization. The controller was simulated, and found usefull for reducing the nonlinearities in the driver. The controller had to be sampled with a larger sampling frequency than first assumed in order to completely remove the harmonics. A Kalman filter was developed as a closed loop observer to estimate the non measurable states of the system. The observer was tested, and found sufficient for this project. The adaptive estimator used a set of coefficients obtained from a Klippel Analyzer to extrapolate the parameters. Methods for estimating the nonlinear parameters of the driver are presented.
The final simulation with the controller and closed loop observer, showed it was not possible to remove the nonlinearities of the driver, but it was proves possible to reduce them.

AALBORG UNIVERSITET

Afdelingen for Elektroniske Systemer
Fredrik Bajers Vej 7C
Telefon 96 35 87 00
Fax 98 15 17 39
http://www.control.aau.dk

Titel:
Compensation of Loudspeaker Driver Nonlinearities Using Predictive and Feedback-Based Approaches

Projekt periode:
September 2007 - Juni 2008

Gruppe:
1035

Medlemmer:
Heine Falkesgaard
Michael Yde Hundsdahl

Vejleder:
Jakob Stoustrup

Kopier: 5

Sider: 85

Appendiks: 4

Afsluttet: 4. juni 2008

Synopsis:

Denne afhandling behandler problemet med ulinearitet i en højtaler enhed. Hypotesen er følgenden: Kan de harminiske forstyrrelsen i en højtaler enhed fjernes ved hjælp af viden om kontrol. Enheden er studeret og en matematisk model er analyseret og reduceret. For at fjerne de harmoniske forstyrrelser er modellen i denne afhandling blevet analyseret og fundet de ulineare elementer der laver de harmoniske forstyrrelser. Et kontrol plan er presenteret og designet.
Planen består af en kontroller, en lukket sløjfe observator og en adaptiv estimater. Den designede kontroller, bruger ulinear kontrol typen feedback linearisering. Kontrolleren er simuleret og fundet brugbar til at reducere ulineariteten i enheden. Kontrolleren skulle samples med en større samplings frekvens en først forventet, for at helt at kunne fjerne de harmoniske. Et Kalman filter var udviklet som en lukket sløjfe observer for at estimere de tilstande af systemet der ikke er målt. Observeren blev testet og fundet tilstrækkelig til dette projekt. Den adaptive estimater bruger et sæt af koefficienter, fundet ved hjælp af en Klippel Analyzer, til at finde parametrene. Metoder til at estimere de ulineare parameter for en enhed er præsenteret.
Den afsluttende simulering med kontroller og lukket sløjfe observer, viste at det ikke var muligt at fjerne lineariterne i enheden, men det var vist at det er muligt at reducere dem.

Preface

The work presented in this thesis has be carried out by group 1035, during the 9th and 10th semester at Automation & Control at the Department of Electronic Systems at Aalborg University.

The report is a master thesis, which has been made on the behalf of Bang & Oulfsen (B&O). We would like to thanks the people at B&O, Sylvain, Gert and Ronnie for the collaboration. We would also like to thanks them for using their facilities and equipment. The reader of this report is presumed to be familiar with modeling of mechanical systems, controlling nonlinear systems.

The report uses the Harvard Reference System, where the reference in the report consists of a (Last name, Year). On page 74 a complete bibliography can be found. In references to tables, figures and equations, the first digit specifies the chapter. For instance; Table 2.1 is the first table in chapter two.

The Matlab software generated in the project, can be required upon request to Heine Falkesgaard, hfal04@control.aau.dk.

Throughout the report the notation driver, refers to loudspeaker driver.

Heine Falkesgaard

Michael Hundsdahl

Contents

List of Acronyms

acc. accelerometer

ADE Adaptive Esitmator

ARE Algebraic Riccati Equation

CLO Closed Loop Observer

DA2 Distortion Analyzer 2

DSP Digital Signal Processor

DFT Discrete Fourier Transform

EKF Extended Kalman Filter

EMF Electro magnetic force

FB Feed Back System

FF Feed Forward System

FT Fourier Transform

FFT Fast Fourier Transform

KF Kalman Filter

KVL Kirkhoff Voltage Law

LMS Least-Mean Square

LTI Linear Time-Invariant

MSE Mean Square Error

NSSM Nonlinear State Space Model

RMS Root Mean Square

SVD Singular Value Decomposition

UKF Uncented Kalman Filter

List of Figures

CHAPTER 1

Introduction

The topic of this thesis is Compensation of Loudspeaker Driver Nonlinearities, a topic that has been treated for many years.

A driver is a transducer that converts the electrical signal from an amplifier to sound. The signal influence the voice coil which is connected to the diaphragm thereby producing sound. The movement of the voice coil is not linear. When the voice coil is in an outer position more current is needed to move the coil a small distance. This makes the driver a nonlinear system.

To overcome the nonlinearities of the driver, acoustic knowledge is used to optimize the performance of the driver, a linear model is used. This can be a correct estimation in some cases, but since the driver is nonlinear, this estimation is not completely correct.

In the later years, a new approach is tested, using control knowledge to compensate for the nonlinearity of the driver and thereby improving the sound experience. Using adaptive and feed back-based approaches there can be compensated for the nonlinearities of the driver. This thesis will examine this by designing a compensator and an estimator for the system. These will be analysed as a proof of concept, and there will be concluded on a controller as a way of removing the driver nonlinearities.

The driver is provided by B&O. The driver is a Tymphany-Peerless S07-215. The driver used for testing is a bass unit. This type of driver has a larger excursion of the voice coil. The driver is intended mounted in an enclosed box, which will be used when designing the mathematical model. A bass driver operates in the lower frequencies, the frequency band will be limited to 20 Hz to 300 Hz.

The scope of this thesis is to investigate an approach for solving the problem with the nonlinearity in the driver. There will be described three different control methods, two different control methods and the third a combination of the two. In the following the three methods will be described but only one of them will be designed and used in this thesis. In the end of this thesis, simulation and test will determine if a controller is a valid method for optimising the driver.

The controller will be implemented before the driver and amplifier, see Figure 1.1.

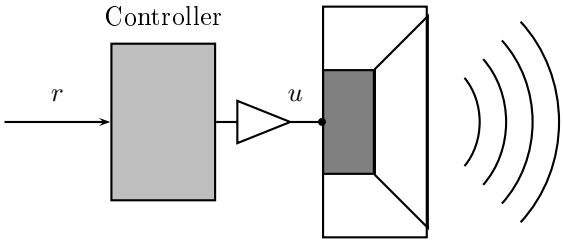

Figure 1.1: *The system, with the controller implemented.*

1.1 Feed Back Control

The Feed Back System (FB) will control the dynamic behavior of the driver. The FB will consist of a controller and a sensor. The sensor is mounted on the driver and will measure the excurstion of the voice coil. The excursion of the voice coil will be fed back to the reference signal and used in the controller to correct for the nonlinearities. By using this approach the nonlinearity can be found, and taken into consideration using the FB, see Figure 1.2.

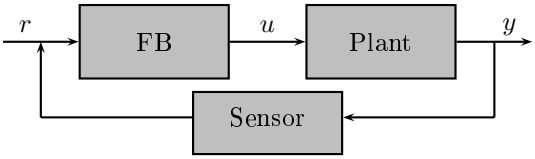

Figure 1.2: *Concept structure of a feed back control system.*

By using this approach an accelerometer could be used. It is an inexpensive method but has the disadvantage of mounting the sensor on the driver, and the robustness of it. The advantage of the FB is that a closed loop is achieved which improves the stability of the system.

1.2 Adaptive Control

A second approach to controlling the excursion of the driver, is to make a mathematical model of the system. By using the model to predict the output, there can be a compensation for nonlinearities. In order to do this, the parameters of the physical speaker has to be measured and used in the model.

By measuring the current used in the driver the controller updates the model parameter and adjust the input signal to the present state of the driver. The adaptive control is shown in Figure 1.3.

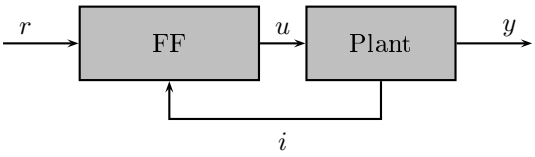

Figure 1.3: *Concept structure of a adaptive control system.*

The current used as input signal for the control, is easy measured using a resistor. The cost of this method is preferable. The robustness and linearity is also an advantaged(Klippel, 1999). Due to Electro magnetic force (EMF) detection and calculation of the model, some kind of signal processing is needed. An option could be a Digital Signal Processor (DSP).

1.3 Adaptive Feed Back Control

The third control method described, is a combination of the two previous explained control methods. By using FB and adaptive control, the accuracy of the controller could be improved. Figure 1.4 shows such a control strategy.

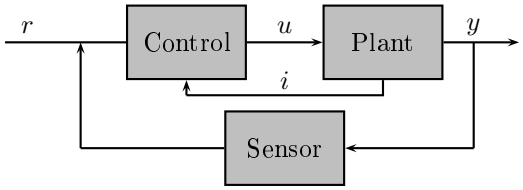

Figure 1.4: *Concept structure of an adaptive feed back control system.*

1.4 Chosen Control Method

It is chosen to use the adaptive control, using current measurement for prof the concept of this thesis. It is chosen because the measurement of the current can be done using simple measurement devices and no modification of the driver is needed.

In the next section the procedure for this thesis and the solution for the problem is presented.

1.5 Overview of the Report

The overview is made to give the reader an idea of how the report is structured, and the steps taken to prove the concept.

Chapter 2 - Design of Driver In this chapter there will be given a general overview of the driver. The driver will be analysed and a mathematical model is presented.

Chapter 3 - Nonlinearities of Driver The driver is a nonlinear system. The parameters making the driver nonlinear is introduced in this chapter.

Chapter 4 - Analysis of Harmonic Distortion It is chosen to use the harmonic distortion as a way of determine the improvement of the designed control scheme. In this chapter the harmonic distortion is described and a way of measuring is introduced.

Chapter 5 - Model Analysis The model is analysed in this chapter. The model is reduced due to unnecessary elements. A linear and nonlinear model are compared to verify the reduced model. The controllability and observability is determined.

Chapter 6 - Control Scheme for driver The control scheme for the adaptive feedback control is explained in this chapter.

Chapter 7 - Measurement Block In this chapter the measurement block in described.

Chapter 8 - Closed Loop Observer This chapter introduces the Kalman filter as the closed loop observer, to estimate the states of the system. First the general form followed by the discrete extended Kalman filter which is used on nonlinear systems. The Extended Kalman filter is applied to the system and verified.

Chapter 9 - Nonlinear Control The nonlinear control is described in this chapter. The system is linearized and the compensator is designed.

Chapter 10 - System Identification Three ways of identifying the parameters of the driver is described in this chapter. The three methods are Mean Square Estimate, Singular Valued Decomposition and Kalman Filter. The System Identification is only described and not implemented.

Chapter 11 - Results of Compensation of Driver In this chapter the compensator is tested on the simulated driver.

Chapter 12 - Conclusion and Future Work In this chapter the conclusion of the control scheme is described and the future work for this thesis is introduced.

CHAPTER 2

Design of Driver

This chapter will describe the construction of a driver, by clarifying which components the driver consists of. There will also be a description of modeling a driver.

In order to describe the construction of the driver, the components will be investigated. These components will be used for modeling the driver.

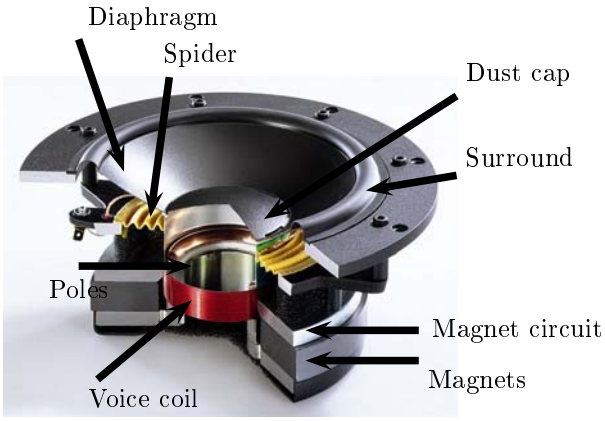

Figure 2.1: *Cut-away view of a dynamic driver.(Technology, 2007)*

2.1 Construction

The driver consist of several components which in combination makes the driver. In Figure 2.1 a cut-away picture of a driver is shown, this is used for illustration. The sound from the driver starts with a voltage applied through two terminals. These terminals are connected to the *magnetic*

circuit. Inside the *magnetic circuit*, a *magnet* is placed. When the electrodynamic signal is applied a force between the *magnet* and the surrounding circuit is made, which influence the *voice-coil* to move.

The lower part of the *voice-coil* is located inside this area of force generated by the *magnet* and the surrounding area. The upper part of the *voice-coil* is attached to the *diaphragm*. The *diaphragm* moves vertical, which generates a sound pressure.

The *spider* is mounted to the frame and the *voice-coil* is used as suspension. There are two functions of the *spider*. The main purpose is to provide the restoring force factor (compliance, which is the reciprocal to the stiffness) for the speaker. The stiffness of the *spider* determines the speakers resonance. The resonance of the speaker is a function of the compliance and the mass of the loudspeaker.

$$f_s = \frac{1}{2\pi}\sqrt{\frac{1}{C_B \cdot M_D}}, \tag{2.1}$$

where f_s is the driver free air resonance frequency, C_B is the driver compliance, M_D is the total mass of the driver (the weight of the entire cone assembly, voice coil, cone, spider and surround, plus free-air air mass load). The resonance frequency will shift to a lower frequency when a small

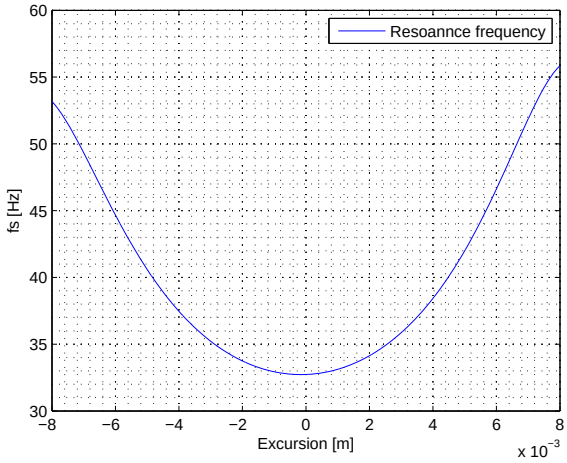

Figure 2.2: *The resonance frequency, as a function of the excursion.*

input signal is applied to the driver. A possible explanation of the change in resonance frequency is when a small signal is applied, the excursion of diaphragm is small which increases the compliance, and as shown in (2.1) decreases f_s, see Figure 2.2.

The secondary task for the *spider* is to keep the voice coil centered over the *pole piece* and keep foreign particles away from the gap area.

The *surround* also have two jobs. Its primary job is to keep the *voice coil* centered over the *pole piece*, and damping the vibration at the outer edge of the cone. The *surround* provides about 20% of the compliance for the speaker (Dickason, 1997, p. 3-9).

2.2 Modeling

After the drivers construction has been discovered in the last section, an analogue of the driver will be derived. The achieved model of the driver will be used in the later sections for control purpose. The model is made by analyzing the system and determine the states in the system.

2.2.1 State Equations

An analogues circuit of the driver in an enclosed-box, is shown in Figure 2.3, where it is divided into three parts:

1. Electronic circuit,
2. Mechanical circuit,
3. Acoustical circuit.

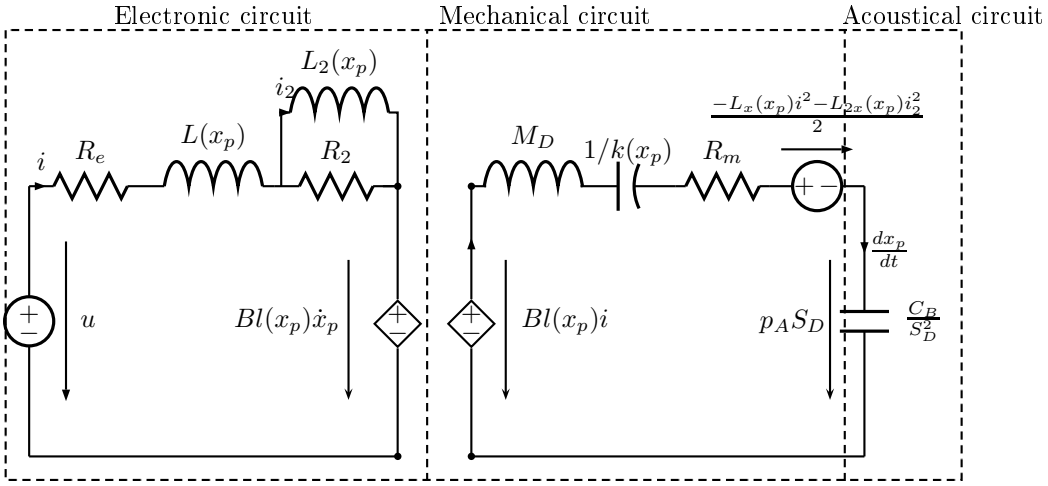

Figure 2.3: *Model of an analogues circuit of an enclosed-box driver system.*

The electrical circuit consists of the input voltage $u(t)$ from an amplifier, a resistant R_e and a inductance $L(x_p)$ representing the resistance of the driver voice coil, and a transformation from the electrical to the mechanical circuit respectively. To compensate for the eddy current (see appendix A on page 75 for further information) generated in the inductance of the voice coil, a small circuit, consisting of a resistance R_2 parallel coupled with a inductance $L_2(x_p)$, is inserted. The controlled voltage supply to the mechanical part, $Bl(x_p)\dot{x}_p$ is represented by the diamond shaped figure.

The mechanical circuit is represented by an inductance M_D representing the mechanical mass of the diaphragm assembly, a conductance $1/k(x_p)$ representing the compliance of the driver suspension, a resistant R_m representing the mechanical resistance of the total driver losses, and a voltage generator representing the reluctance force caused by the nonlinear self inductance and the displacement-dependent stiffness of the spider (Hans Schurer and Herrmann, 1998, p. 2).

The acoustical circuit is represented by a conductance, $\frac{C_B}{S_D^2}$. The conductance is representing the compliance of the air in an enclosed box. The components from Figure 2.3, where S_D is the effective surface area of the diaphragm, are describe in Table 2.1 on the next page.

Inspecting Figure 2.3, the following equations can be derived from the analogue of the driver.

$$u(t) = R_e \cdot i(t) + \frac{d\left(L(x_p)i(t)\right)}{dt} + R_2(i(t) - i_2(t)) + Bl(x_p) \cdot \dot{x}_p \tag{2.2a}$$

$$R_2 \cdot (i(t) - i_2(t)) = \frac{d\left(L_2(x_p)i(t)\right)}{dt} \tag{2.2b}$$

$$\frac{dx_p}{dt} = \dot{x}_p \tag{2.2c}$$

$$Bl(x_p) \cdot i = M_D\ddot{x}_p + k(x_p) \cdot x_p + R_m \cdot \dot{x}_p - \frac{L_x(x_p) \cdot i^2}{2} - \frac{L_{2x}(x_p)i_2^2}{2} + \frac{S_D^2}{C_B(x_p)}x_p \tag{2.2d}$$

Table 2.1: *Components of Figure 2.3 on the previous page.*

Factor	Description	Unit
	Electronic circuit	
R_e	Electrical voice coil resistance (at DC).	$[\Omega]$
$L_e(x_p)$	Instantaneous inductance of voice coil.	$[H]$
$Bl(x_p)$	Instantaneous force factor.	[N/A]
$L_2(x_p)$	Para inductance of voice coil, due to eddy current.	$[H]$
R_2	Electrical resistance, due to eddy current.	$[\Omega]$
	Mechanical circuit	
M_D	Mechanical mass of diaphragm assembly, including voice coil and air load.	[kg]
$k(x_p)$	Instantaneous stiffness of suspension.	[N/m]
R_m	Mechanical resistance of total driver losses.	[kg/s]
	Acoustical circuit	
$C_B(x_p)$	Acoustic compliance of air in enclosure	[m/N]
S_D	Surface area of the diaphragm	$[m^2]$

where $L_x(x_p)$ is the first order derivative of $L_e(x_p)$, and $L_{2x}(x_p)$ is the first order derivative of $L_2(x_p)$. Equation (2.2b) is found from the eddy current circuit, knowing the voltage over the resistant and inductor is equal. Equation (2.2a) and (2.2d) are derived using Kirkhoff Voltage Law (KVL) in the mechanical and electrical circuit.

The nonlinear equations listed from (2.2a) to (2.2d) are written as a vector field of the form

$$\begin{aligned} \dot{x} &= f(x) + g(x)u \\ y &= h(x) \end{aligned} \tag{2.3}$$

where $u \in \mathbb{R}$ is the voltage applied to the driver, $y \in \mathbb{R}$ is the output corresponding to the excursion $x_p(t)$ of the diaphragm. The functions $f(\cdot)$ and $g(\cdot)$ is assumed to be smooth, and $h(\cdot)$ is a column of smooth function of the state vector x. The state vector in the system are chosen

$$x = \begin{bmatrix} x_1 & x_2 & x_3 & x_4 \end{bmatrix}^T = \begin{bmatrix} i & i_2 & x_p & \dot{x}_p \end{bmatrix}^T \tag{2.4}$$

where i is the current in the driver, i_2 is the current through L_2, x_p is the excursion of the voice coil, and $\dot{x}_p$ is the velocity of the excursion of the voice coil.

From (2.2a) to (2.2d) a continuous vector field can be derived, where

$$\begin{aligned} f(x) &= \begin{bmatrix} \frac{1}{L_e}\left(\left(-R_e - R_2\right)x_1 + R_2 x_2 + \left(-L_x x_1 - Bl\right)x_4\right) \\ \frac{1}{L_2}\left(R_2 x_1 - R_2 x_2 - L_{2x} x_2 x_4\right) \\ x_4 \\ \frac{1}{M_D}\left(\left(\frac{1}{2}L_x x_1 + Bl\right)x_1 + \frac{1}{2}L_{2x}x_2^2 + \left(-k - \frac{S_D^2}{C_B}\right)x_3 - R_m x_4\right) \end{bmatrix} \\ g(x) &= \frac{1}{L_e} \\ h(x) &= x_3 \end{aligned} \tag{2.5}$$

where the nonlinear parameters, L_e, Bl, k, L_x, L_{2x} is all a function of the excursion, x_3. The vector filed is nonlinear hence the current in the reluctance, and some parameters are found to be nonlinear, see chapter 3 for further information.

This thesis will only investigate the influence directly at the driver, and not the driver mounted in an enclosed box. Since the interest is the driver, the modeling of the driver is equal to modeling in a infinity large enclosed box, and thereby the acoustical part $\frac{S_D^2}{C_B}$, can be left out.

To solve the differential equations, the Runge-Kutta algorithms can be used. Using this algorithms the continuous nonlinear equations can be converted to discrete nonlinear equations, which is preferable due to the implementation method. Runge-Kutta is an explicit iterative method of approximating a solution for a differential equation. Approximating the next value is done by evaluating the present value and the derivatives of this.

It is chosen to use the less sophisticated version of Runge-Kutta - the Forward Euler method. The method is chosen since the expectation of the remaining derivatives of the outcome will not change by using the classical Runge-Kutta algorithm. The Forward Euler algorithm is defined as (Kreysig, 1999):

$$X(n+1) = X(n) + T_s \cdot \frac{dX(n)}{dt} \Leftrightarrow \frac{dX}{dt} = \frac{X(n+1) - X(n)}{T_s} \tag{2.6}$$

where T_s is the samplings frequency. T_s has to be at least five times higher than the frequency of the signal.

The discrete nonlinear state space model is written as:

$$x(n+1) = Fx(n) + Gu(n) \tag{2.7}$$
$$y(n) = Hx(n) \tag{2.8}$$

where n is sampling to present time, F is the time varying matrix, G is the time varying input vector and H is the measurement matrix.

The matrix and vector for the state space model yields

$$\begin{aligned} F &= \begin{bmatrix} \left(1 + \frac{T_s}{L_e}(-R_e - R_2)\right) & \frac{T_s}{L_e}R_2 & 0 & \frac{T_s}{L_e}\left(-L_x x_1(n) - Bl\right) \\ \frac{T_s}{L_2}R_2 & \left(1 - \frac{T_s}{L_2}R_2\right) & 0 & -\frac{T_s}{L_2}L_{2x}x_2 \\ 0 & 0 & 1 & T_s \\ \frac{T_s}{M_D}\left(\frac{L_x x_1}{2} + Bl\right) & \frac{T_s}{M_D}\left(\frac{L_{2x}x_2}{2}\right) & -\frac{T_s}{M_D}k & \left(1 - \frac{T_s}{M_D}R_m\right) \end{bmatrix} \\ G &= \begin{bmatrix} \frac{T_s}{L_e} & 0 & 0 & 0 \end{bmatrix}^T \\ H &= \begin{bmatrix} 0 & 0 & 1 & 0 \end{bmatrix} \end{aligned} \tag{2.9}$$

After the fundamental equations describing the driver and a discrete time version of the driver has been presented, the parameters for the driver will be described.

CHAPTER 3

Parameters of Driver

In section 2.2 the model of the driver where constructed. Several parameters where introduced and in this chapter the most pivotal parameters will be analyzed and their influence will be described. The pivotal parameters is the parameters which changes the most during use of the driver.

Operating the driver in a way, where the excursion of the voice coil is little, the drivers amplitude response stay linear. But when the excursion of the voice coil increases the time response of the driver becomes nonlinear.

When the driver is operating, a distortion occurs. This occurs because the excursion of the diaphragm is limited. As mention in section 2.1 on page 19 the diaphragm is connected to the surround which limits the movement of the diaphragm.

The parameters which is dependent on the voice coils excursion are referred as the nonlinear parameters and described here:

$Bl(x_p)$ instantaneous electrodynamic coupling factor (force factor of the motor) defined by the integral of the magnetic flux density B over voice coil length l,

$k(x_p)$ mechanical stiffness of driver suspension,

C_B mechanical compliance of driver suspension (the reciprocal of stiffness $k(x_p)$), $1/k(x_p)$,

$L_e(x_p)$ part of voice coil inductance which is independent on frequency.

In the following section the nonlinear parameters are described in detail.

3.1 Nonlinear Parameters

The nonlinear behavior of the driver is caused by a number of elements. In the following these elements are describe to clarify the effects of the nonlinearities.

3.1.1 Force Factor

The force factor, $Bl(x_p)$ describes the coupling between the electrical and the mechanical part of the driver. The parameter is the integral of the flux density B over the length of the voice coil l, $\int B(l)dt$. The force factor is modeled by a fourth order polynomial approximation

$$Bl(x_p) = bl_0 + \sum_{i=1}^{4} bl_i x_p^i \tag{3.1}$$

where bl_0 is a linear component, and $bl_1 - bl_4$ are the nonlinear coefficients.

In Figure 3.1 an overhang configuration of the coil is shown. The construction of a voice coil are

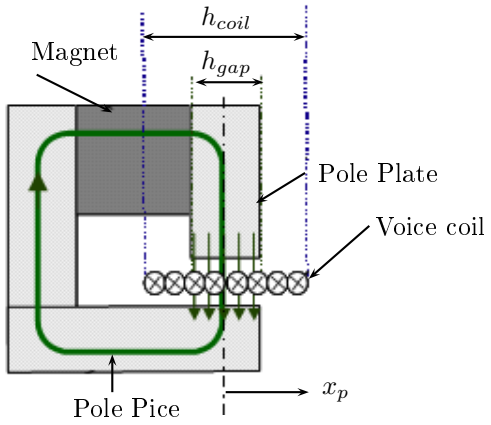

Figure 3.1: *Motor structure of an overhang configuration.*

divided into two types, an overhang voice coil, and an underhung voice coil. The relationship between the two types are describe as

$$\text{overhang} = h_{\text{coil}} > h_{\text{gab}} \tag{3.2}$$

$$\text{underhung} = h_{\text{coil}} < h_{\text{gab}} \tag{3.3}$$

where h_{coil} is the height of the voice coil, and the h_{gab} is the size of the magnet. An underhung voice coil has a more linear, response than an overhang over short distance, but has a lower force factor. An overhang voice coil is more preferable because of its good linearity and efficiency (Dickason, 1997).

The parameter is dependent on the position of the voice coil - when the voice coils windings are leaving the gap, the force factor decrease. A sketch of the force factor as a function of the excursion is shown in Figure 3.2 on the next page.

This parameter has two nonlinear effects.

1. The coupling between the electrical and mechanical domain a variation of $Bl(x_p)$ will change the electro-dynamic force $F_{ed} = Bl(x_p) \cdot i(t)$. This is also known as parametric excitation of a resonating system. Large values of x_p and current $i(t)$ are required to produce significant distortion.

2. EMF generated by the movement of the voice coil is changed when the $Bl(x_p)$ is changed. This force is $F_m = Bl(x_p) \cdot \dot{x}_p$, which causes variation of the electrical damping(Klippel, 1998).

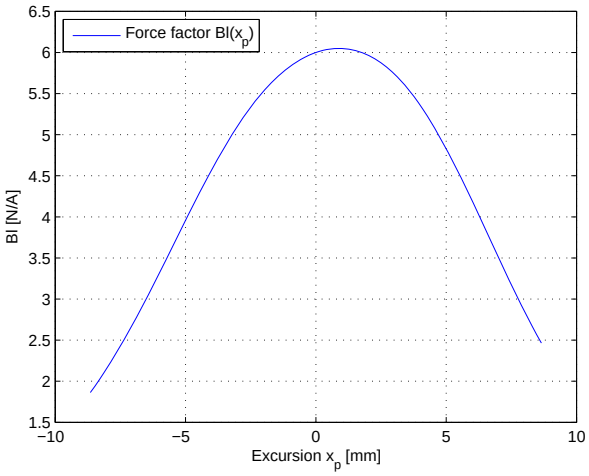

Figure 3.2: *The force factor, $Bl(x_p)$ as a function of the excursion of the coil.*

3.1.2 Stiffness Factor

The suspension of the driver, as described in chapter 2 on page 19, is designed to keep the voice coil centered. The fabric for the suspension can be different depending on the driver which lead to different behaviors. The behavior of the suspension is like a normal spring, and characterized as a force-deflection curve, as shown in Figure 3.3. At low excursion the suspension is almost linear, but

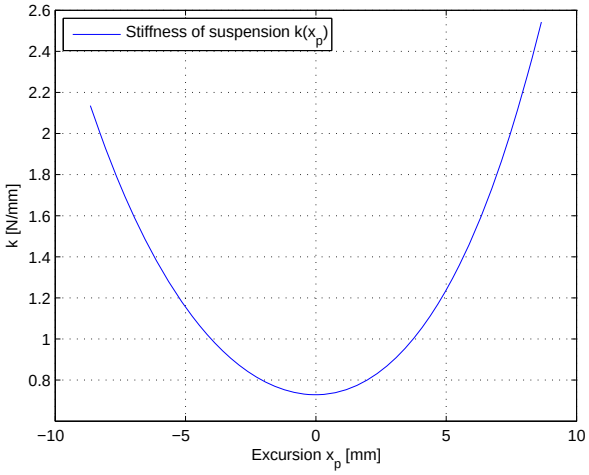

Figure 3.3: *The stiffness factor $k(x_p)$ as a function of the excursion.*

when the excursion increases the suspension reacts with more force than a linear spring, showing that the suspension is nonlinear.

The stiffness parameter, $k(x_p)$, is modeled by a fourth-order polynomial approximation

$$k(x_p) = k_0 + \sum_{i=1}^{4} k_i x_p^i \tag{3.4}$$

where k_0 is a linear component, and $k_1 - k_4$ are the nonlinear coefficients.

The corresponding force $F_k = k(x_p)x_p$ is a product of the excursion x_p and the nonlinear stiffness $k(x_p)$. The stiffness corresponds with the secant between any point of the force-reflection curve and the origin. Since the force is nonlinear it produces a nonlinear distortion in the time signal, which is typical for the suspension. The stiffness also varies as a function of frequency due to visco-elastic behavior of the suspension material. As mentioned earlier the compliance is reciprocal of the stiffness, $C_B(x_p) = 1/k(x_p)$.

3.1.3 Voice Coil Inductance

The electric input impedance depends on the position of the voice coil. The electrical impedance is higher for the negative excursion than the positive excursion (open air). This property is caused by the magnetic flux that depends on the position of voice coil and magnitude of the current. If the coil is placed in open air the inductance is much smaller than if the coil is operating below the gap, where the surrounding material decreases the magnetic resistance. The voice coil inductance is shown in Figure 3.4.

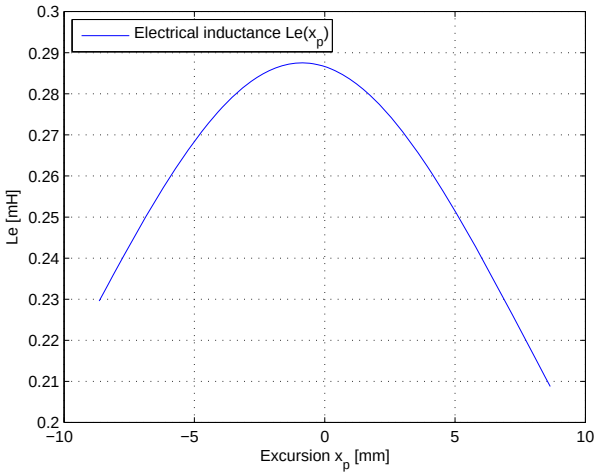

Figure 3.4: *The voice coil induction, $L_e(x_p)$ as a function of the excursion.*

The voice coil inductance, $L_e(x_p)$, is model as a fourth-order polynomial approximation

$$L(x_p) = l_{e0} + \sum_{i=1}^{4} l_{ei} x_p^i \tag{3.5}$$

where l_{e0} is the linear component, and $l_{e1} - l_{e4}$ are the nonlinear coefficients.

The inductance also depends on the input current $i(t)$, this is caused by the nonlinear relationship between the magnetic flux density and the magnetic field strength H ($B = \mu(i(t))H$).

The reluctance force, which drives the mechanical system directly, can be approximated by(Klippel, 1999)

$$F_m(x_p, i, i_2) = -\frac{i(t)^2}{2}\frac{dL(x_p)}{dx} - \frac{i_2^2(t)}{2}\frac{dL_2(x_p)}{dx} \tag{3.6}$$

$$= -\frac{L_x \cdot i^2}{2} - \frac{L_{2x} \cdot i_2^2}{2}. \tag{3.7}$$

3.2 Temperature Parameter Drifting

Mentioned in chapter 1 on page 15 the parameters in a driver may vary due to temperature. This section will clarify the influence of the temperature change on the parameters of a driver. The results were described in (Pedersen and Rubak, 2007), where a series of drivers have been tested.

In the paper, the drivers where tested in the range of 20 to 50°C. Afterward the result was compared to a test performed by (Krump, 1997).

The results of the two tests are shown in Table 3.1. Analyzing the results of the two tests,

Table 3.1: *Temperature drifts of linear parameters, where second column is the (Krump, 1997) test, and the third column is the (Pedersen and Rubak, 2007).*

Parameter	Change, (20 to 80°C)	Change, (20 to 50°C)
Voice Coil resistance, R_e	20%	11%
Force Factor, Bl	-13%	-6%
Moving mass, M_D	-10%	-3%
Suspension compliance, C_B	-9%	-21%
Mechanical resistance, R_m	-42%	-20%

clarifies the change in electrical resistance R_e is significant, 20% and 11%, with the different final temperature it is assumed to be the same.

The change in value of R_e due to temperature is modeled as

$$R_e(T) = R_e(T_0)\,(1 + \alpha(T - T_0)) \tag{3.8}$$

where $\alpha = 4.33{\cdot}10^{-3}\ \mathrm{K}^{-1}$ for copper. The linear relationship of R_e as a function of the temperature is shown in figure 3.5.

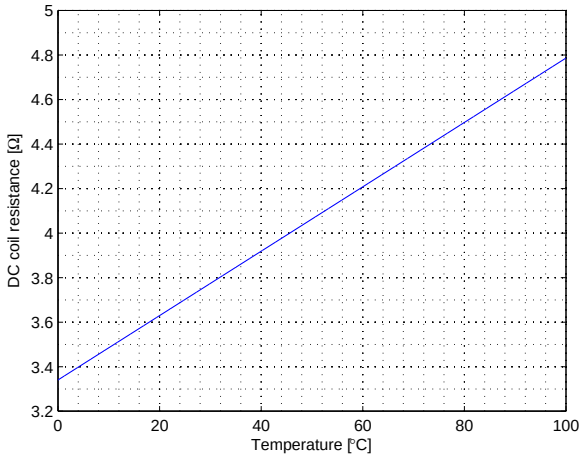

Figure 3.5: *DC coil resistance R_e as a function of the temperature.*

The greatest variation is regarding the compliance C_B, and the mechanical resistance R_m, because the mass is the most stable parameter. The variation in the passive mechanical system are more equally distributed between C_B and R_m in the test performed by (Pedersen and Rubak, 2007).

The drivers linear parameters is found to be drifting relative much, but the drift of the nonlinear parameters are relative small. This is documented in (Bright, 2002) and (Klippel, 1999).

The drifting of the parameters is worth taking into consideration when making a model of the driver. Not only the nonlinear parameters change value. Over a longer period of time the linear parameters will also change.

3.3 Parameter Values

Now the parameters have been described for the model. In order to test the model, parameter values have been found for this purpose. These are found on B&O using a Klippel Analyzer. The Klippel Analyzer, see appendix C for further information, is able to run a driver through numerous of tests, meanwhile measuring the position of the diaphragm. Analyzing these measurements produces a full set of parameters for the driver, linear and nonlinear. The values obtained for the loudspeaker used in this project, is shown in table 3.2. The nonlinear parameters are given at $x_p = 0$.

Table 3.2: *Parameter values used for the driver.*

Parameter	**Value**	**Unit**
R_e	3.34	Ω
R_2	1.70	Ω
R_m	1.582	kg/s
M_D	0.0175	kg
$L_e(x_0)$	0.29	mH
$L_2(x_0)$	0.80	mH
$C_B(x_0)$	1.37	mm/N
$Bl(x_0)$	6.08	N/A

CHAPTER 4

Analysis of Harmonic Distortion

As described earlier the driver generates harmonics waves which are to be canceled out by the controller. To investigate the harmonics generated in the driver a method has to be made. In this thesis the method chosen to analyse the harmonic distortion is the radiated power of the excursion. By use of this method the harmonics can easily be shown.

4.1 Harmonic Tones

The harmonic tones, which are generated in a driver, is unwanted due to its influence on the sound quality. An orchestra playing is not reproduced correctly when played through a loudspeaker. The sound is altered, due to the structure of the driver. The driver structure effects the sound in such a way that there is generated distortion. The distortion generated is called harmonics, and consists of the fundamental tone periodic repeated - saying a 440 Hz tone is played. The second order harmonic is generated at 880 Hz and the third at 1320 Hz and so on. These harmonic are not wanted in the a sound system. The harmonics can generate unknown distortion that can be heard by some humans.

A method to locate these harmonics needs to be designed. In this thesis it is chosen to locate the harmonics by analysing the radiated power of the excursion. The sound pressure generated by the voice coil movement should be pure, if the sound from the driver is not contaminated by distortion.

4.2 Radiated Power of Excursion

The radiated power of excursion can be expressed as

$$P_{AR} = \frac{1}{2}\frac{\rho_0 \omega^2}{4\pi c}\|U\|^2 \tag{4.1}$$

where ρ_0 is the density of the air (assumed 1 for the atmospheric air), c is the velocity of light, ω is the frequency, U is the velocity of the volume(W. Marshall Leach, 1998).

Since the power of the excursion is a function of the frequency, and the voice coil is expressed as a function of time, the transformation from the time domain to the frequency domain must be made. For this transformation the Fast Fourier Transform (FFT) method is used. The FFT method uses the Cooley-Tukey algorithm to decompose the problem of computing the Discrete Fourier Transform (DFT) of the signal. For the FFT method the Hanning window is used. The window is applied to the time-sampled signal and there after the FFT is made. The window causes the Fourier Transform (FT) to have non-zero values at the frequencies of interest, ω_0. The window also have the highest amplitude at ω_0 and the lowest far from ω_0. The Hanning window uses the discrete probability mass function given by

$$\omega(n) = 0.5 \left(1 - \cos\left(\frac{2\pi n}{N-1}\right)\right) \tag{4.2}$$

where N is the length of the sampling. The Hanning window is chosen due to the use of a rectangular windows performance. The rectangular windows performance decreases if the input signal contains some random noise close to the frequency, since the response to noise, compared to the sinusoid will be higher. Hanning window is commonly used in narrow-band applications, and since the driver range is between 20-300 Hz this is preferable, the responds to noise compared to the sinusoid will be more justified.

CHAPTER 5

Model Analysis

In this chapter the model is analysied, to locate the proper size of the states, and verify that the model is comparable to the real driver used in this project.

5.1 Model Simulation

The driver is analysed in order to see the behavior of the system, such that the preference for the controller is known. The analysis is also performed to see if the model behave unexpected, and to locate if there is some special characteristic behavior that needs to be taken into consideration.

The analysis is made by setting the initial excursion of the voice-coil to zero, thereby retriving the linear value of the nonlinear parameters.

The linear system is described in the normal form as

$$\begin{aligned} \dot{x} &= Ax + Bu \\ y &= Cx \end{aligned} \tag{5.1}$$

$$\begin{aligned} \dot{x} &= \begin{bmatrix} \frac{1}{l_{e0}}\left(-R_e - R_2\right) & \frac{R_2}{l_{20}} & 0 & \frac{-L_{x0}x_1}{l_{e0}} - \frac{bl_0}{l_{e0}} \\ \frac{R_e}{l_{20}} & -\frac{R_2}{l_{20}} & 0 & \frac{-L_{20}x_2}{l_{20}} \\ 0 & 0 & 0 & 1 \\ \frac{1}{M_D}\left(\frac{1}{2}L_{x0}x_1 + bl_0\right) & \frac{1}{2}\frac{l_{20}x_2}{M_D} & \frac{-k}{M_D} & \frac{-R_m}{M_D} \end{bmatrix} x + \begin{bmatrix} \frac{1}{l_{e0}} & 0 & 0 & 0 \end{bmatrix} u \\ y &= \begin{bmatrix} 0 & 0 & 1 & 0 \end{bmatrix} x \end{aligned} \tag{5.2}$$

The model of the driver is found to be stable since the state matrix is Hurwitz.

To see if the system has any unexpected behavior a bode plot of the system is made. The bode plot of the system is studied a decade before and after the range of interest.

On Figure 5.1 it can be seen that the driver acts as an amplifier with a -53 dB gain at low frequency.

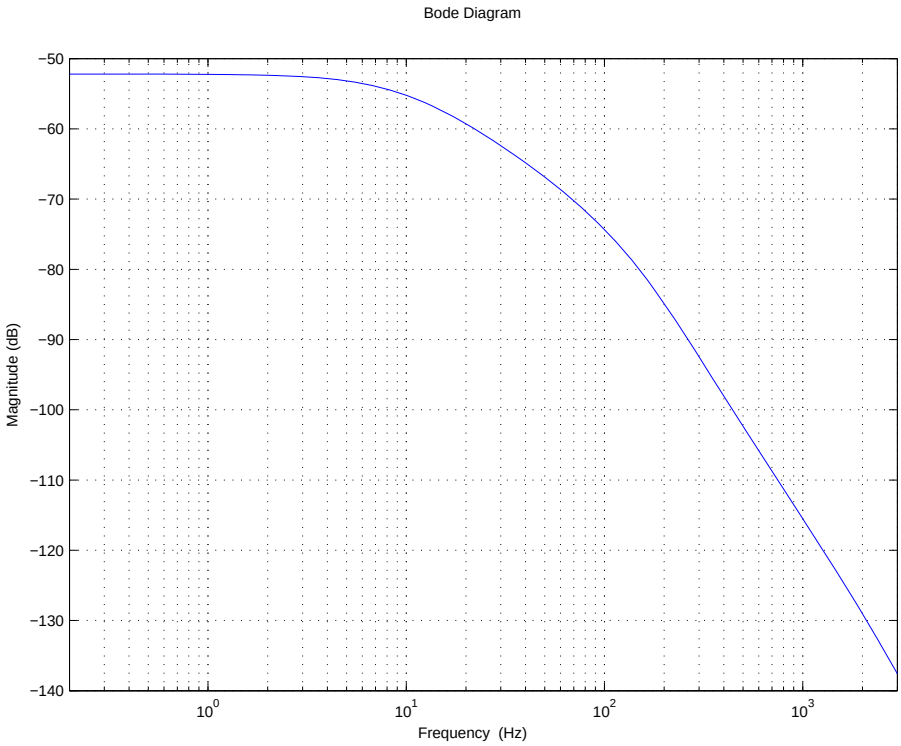

Figure 5.1: *Bode plot of the linear model from 0.2 to 3 kHz.*

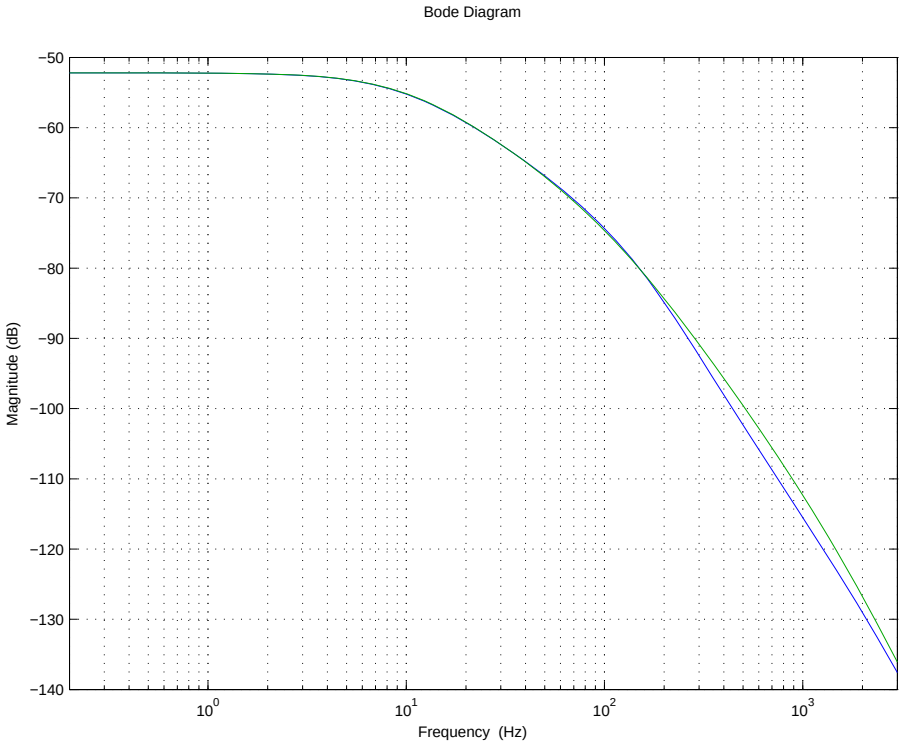

Figure 5.2: *Bode plot of the linear model with (blue) and without (green) the eddy current.*

5.1.1 The Influence of the Eddy Current

Different papers does not take the eddy current into consideration, and therefor the linear system is also evaluated with and without the eddy current, which is shown on Figure 5.2

The influence of the eddy current is shown to be insignificant, since the change of the gain difference at end of the woofer range (300 Hz) is considered small, (approximate 1.5 dB). It is decided that the influence of the eddy current will not affect the model in such way, that the necessity is needed, hence the influence is in the upper range of a woofer.

In Figure 5.3, the error between an impulse response of the linear system with the eddy current applied and without respectively is shown. The result of the plot, shows that the influence for the woofer is significant small, and thereby this thesis does not take the eddy current into consideration.

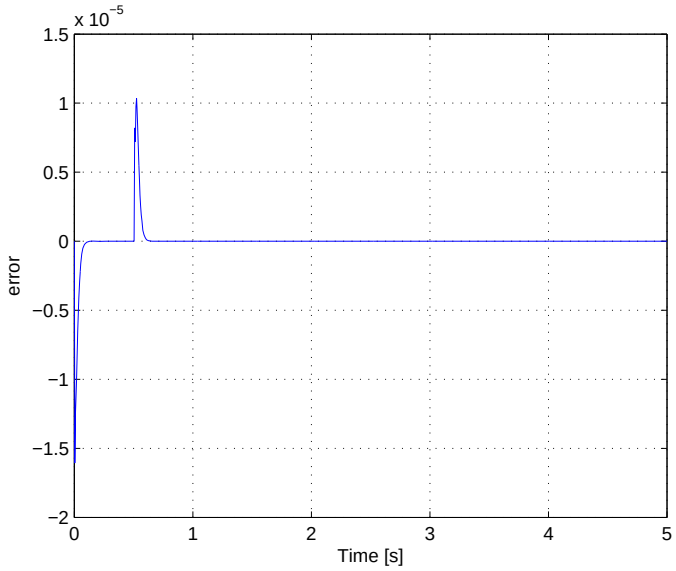

Figure 5.3: *The error between an impulse response of the linear model with and without the eddy current applied respectively.*

5.2 The Reduced Model

Knowing the influence of the eddy current in a woofer is not of relevance, the model is reduce by removing one state. The new model is described as

$$\begin{aligned} \dot{x} &= f(x) + g(x)u \\ y &= h(x) \end{aligned} \tag{5.3}$$

where $x = [x_1 \quad x_2 \quad x_3] = [i \quad x \quad \dot{x}]$

$$\begin{aligned} \dot{x} &= \begin{bmatrix} \frac{-R_e}{L_e}x_1 + \frac{1}{L_e}\left(-L_x x_1 - Bl\right)x_3 \\ x_3 \\ \frac{1}{M_D}\left(\frac{1}{2}\cdot L_x x_1 + Bl\right)x_1 - \frac{1}{M_D}kx_2 - \frac{R_m}{M_D}x_3 \end{bmatrix} + \frac{1}{L_e}u \\ y &= h(x) = x_2 \end{aligned} \tag{5.4}$$

The Nonlinear State Space Model (NSSM) is described as

$$x_{k+1} = Fx_k + Gu_k \tag{5.5}$$
$$y_k = Hx_k \tag{5.6}$$

$$\begin{aligned} F &= \begin{bmatrix} \left(1+\frac{T_s}{L_e}(-R_e)\right) & 0 & \frac{T_s}{L_e}\left(-L_x x_1(n) - Bl\right) \\ 0 & 1 & T_s \\ \frac{T_s}{M_D}\left(\frac{L_x x_1}{2} + Bl\right) & -\frac{T_s}{M_D}k & \left(1-\frac{T_s}{M_D}R_m\right) \end{bmatrix} \\ G &= \begin{bmatrix} \frac{T_s}{L_e} & 0 & 0 \end{bmatrix}^T \\ H &= \begin{bmatrix} 0 & 1 & 0 \end{bmatrix} \end{aligned} \tag{5.7}$$

The reduced model is evaluated at $x_2 = 0$, to located the change in behavior. For the simulation a step is used as input. The excursion is shown in Figure 5.4.

The diaphragm starts at 1 mm, and moves to zero. The movement is smooth and is expected of a driver. After 0.5 seconds a step of two volts is applied for half a second. The diaphragm follows as expected to a fixed position, and follows back to zero when input signal is removed. The diaphragm follows a smooth motion as expected.

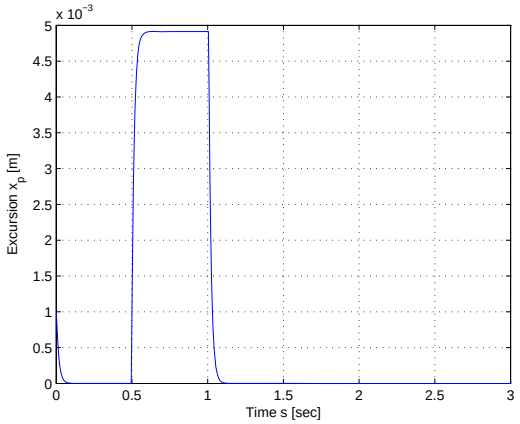

Figure 5.4: *A simulation of a step applied to the linear system.*

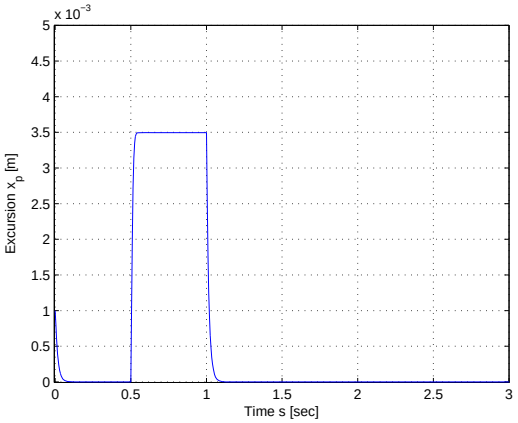

Figure 5.5: *A simulation of a step applied to the nonlinear system.*

5.3 Nonlinear Simulation

For simulating the nonlinear model, the nonlinear parameters is to be adjusted according to the excursion of the voice coil. The values for the parameters used in the simulation are described in section 3.3, and the nonlinear parameters are evaluated as described in appendix D. The reduced model linearized around $x_2 = 0$, is evaluated to see the behavior of the excursion using a FFT analysis method, see figure 5.6. The behavior shows that the harmonic distortion created by the nonlinear parameters is faded out.

For the nonlinear simulation, the function `ode45` in Matlab is used.

The simulation result of the excursion is shown in Figure 5.5. The initial values and input signal from the linear simulation is also used in this simulation. The behavior of the excursion is similar to the previous simulation but is less during the step.

This difference is caused by the varying nonlinear parameters. The change at a 3.5 mm excursion gives a smaller Bl, L_e and C_b and a higher k, which contributes to the smaller excursion than in the linear simulation.

The nonlinear and linear model is similar and the excursion is assumed to be like a real driver. The comparison with a real driver will be done in the next section.

As describe the matlab function `ode45` is used to solve the nonlinear differential equations, and the Forward Euler algorithm has also been described for solving the nonlinear equations. To evaluate the Forward Euler algorithm performance the radiated power of the excursion is inspected for both the outcome of the `ode45` result and the Forward Euler, and are shown in Figure 5.7 and Figure 5.8. The result of the inspection shows that the radiated power for them both are similar, and thereby the Forward Euler algorithm is set to be valid for further use.

5.4 Model Verification

In order to verify the model of the driver is correct, the model is compared against the physical driver.

The verification of the model is done by simulating the excursion of the diaphragm and inspect the harmonic distortion that the nonlinearity creates. The result is compared against the real measurement of the voice-coil excursion and the harmonics that are created in the driver.

The simulation input signal is a 60 Hz sinusoid signal 10 V_{RMS}. The result of the signal is presented in dB for a fair comparison.

5.4.1 Driver - Physical

On Figure 5.9 the power of excursion relative in dB is shown. The measurement is preformed as described in appendix B. The figure shows how the harmonic distortion due to the nonlinear system emerges at every 60 Hz. The amplification of the harmonics are less than the fundamental frequency.

5.4.2 Driver - Model

Figure 5.10 shows that the harmonic distortion occurs in a larger scale than the physical driver. The model and the parameters used in the driver model, is not accurate enough according to the physical driver. The fundamental frequency is about 41 dB less than the real driver. The basic shape of the driver is shown to be the same as the real driver and the model of the driver is concluded to be valid enough for further use.

5.5 Controllability of the Driver

In order to make a controller for the driver, such that the nonlinearity in the driver is faded out, the controllability of the system has to be checked. The controllability theorem for nonlinear systems is defined as follows(Hedrick and Girard, 2005).

The system is defined as

$$\dot{x} = f(x) + \sum_{i=1}^{m} g_i(x)u_i \tag{5.8}$$

is locally accessible about x_0 if the accessibility distribution C span n space, where n is the rank of x and C is defined as

$$C = \left[g_1, g_2, \ldots, g_m, [g_i, g_j], \ldots, \left[ad_{gi}^k, g_j\right], \ldots, [f, g_i], \ldots, \left[ad_f^k, g_i\right], \ldots\right] \tag{5.9}$$

where ad is the Lie Derivative. If $f(x) = 0$ then $\dot{x} = \sum_{i=1}^{m} g_i(x)u_i$ and thereby C has rank n, the system is controllable.

The theorem specifies that, if the nonlinear system is linearized around x_0 and the linearization is controllable, then the nonlinear system is accessible at x_0 - note that if the linearization is uncontrollable the nonlinear system may still be locally accessible.

To determine if the linearization of the system is controllable at x_0 the rank of $\begin{bmatrix} B & AB & \ldots A^{n-1}B \end{bmatrix}$ must be equal to n

$$\begin{aligned} C &= \begin{bmatrix} B & AB & A^2B \end{bmatrix} \\ C &= 3 \end{aligned} \tag{5.10}$$

hence the controllability of the linear system is equal to the number of the states, the nonlinear system is locally accessible.

5.6 Observability of the Driver

To determine how well the internal states of the driver can be inferred by knowledge of the output of the driver, the observability of the driver has to be known. The driver is observable if for any possible sequence of states and control input the current state can be determine in finite time using only the output.

For determine if the driver is locally observable at x_0 there has to exist a neighbourhood of x_0 such that every x in the neighbourhood other than x_0 is distinguishable from x_0.

To establishing that there exist such neighbourhood the following has to be satisfied.

$$O(x_0, u^*) = \left.\frac{\partial l(x_0, u^*)}{\partial x}\right|_{x=x_0} \tag{5.11}$$

must have rank n where n is the rank of x and

$$l(x, u^*) = \begin{bmatrix} L_f^0(h(x)) \\ \ldots \\ L_f^{n-1}(h(x)) \end{bmatrix}. \tag{5.12}$$

For the driver,

$$\begin{aligned} l(x, u^*) &= \begin{bmatrix} h(x) \\ L_f h(x) \\ L_f^2 h(x) \end{bmatrix} = \begin{bmatrix} x_2 \\ \dot{x}_2 \\ \ddot{x}_2 \end{bmatrix} = \begin{bmatrix} x_2 \\ x_3 \\ \dot{x}_3 \end{bmatrix} \\ &= \begin{bmatrix} x_2 \\ x_3 \\ \frac{1}{M_D}\left(\frac{1}{2}L_x x_1 + Bl\right) x_1 - \frac{1}{M_D} k x_2 - \frac{R_m}{M_D} x_3 \end{bmatrix} \end{aligned} \tag{5.13}$$

and the system is locally accessible if

$$O(x_0, u^*) = \begin{bmatrix} 0 & 1 & 0 \\ 0 & 0 & 1 \\ \frac{1}{2M_D}\left(2L_x x_1 + Bl\right) & -\frac{1}{M_D} k & -\frac{R_m}{M_D} \end{bmatrix} \tag{5.14}$$

has rank 3, which is satisfied, thereby the system is local accessible.

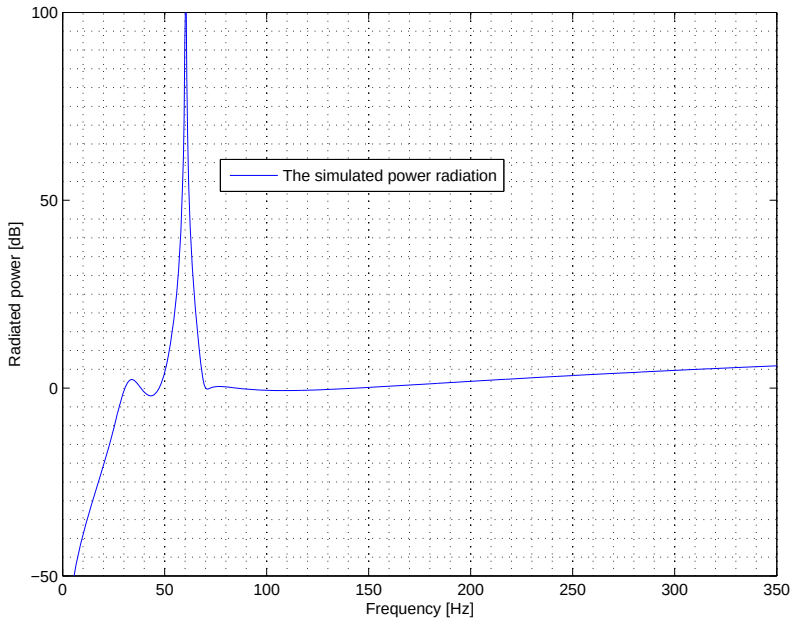

Figure 5.6: *The radiated power of the excurstion, simulated with the linearized model.*

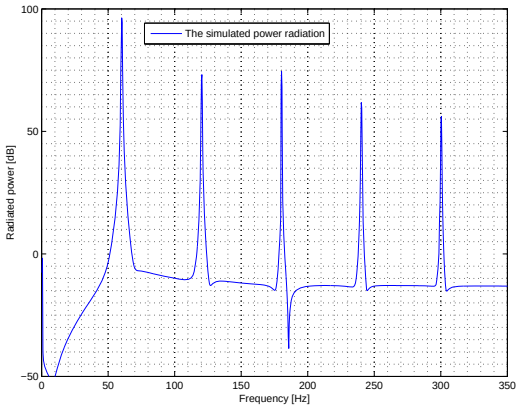

Figure 5.7: *The radiated power simulated by the* `ode45` *function.*

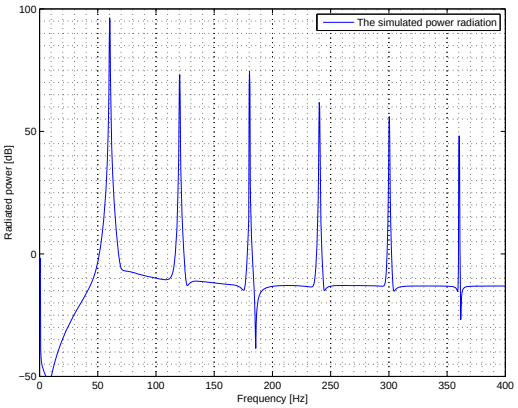

Figure 5.8: *The radiated power simulated by the Forward Euler algorithm.*

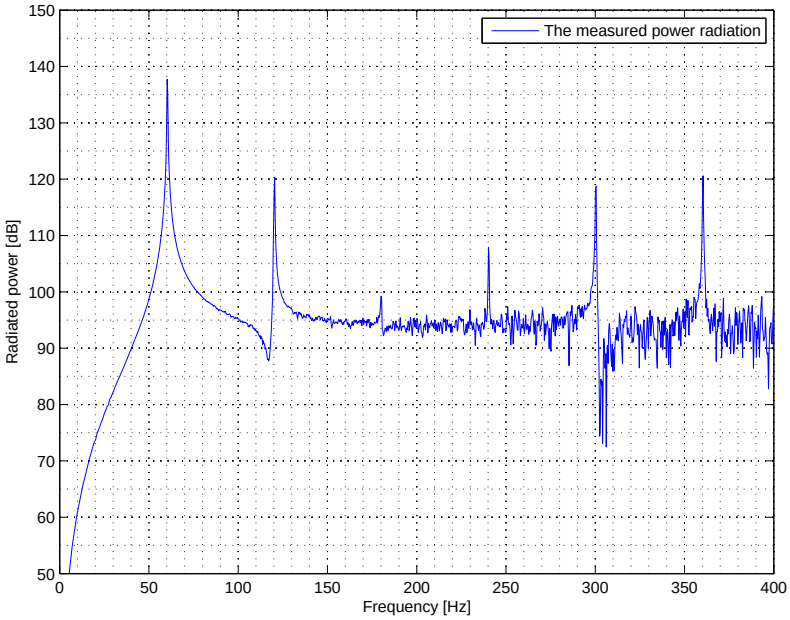

Figure 5.9: *The radiated power of the physical driver with a sinusoid signal at 60 Hz.*

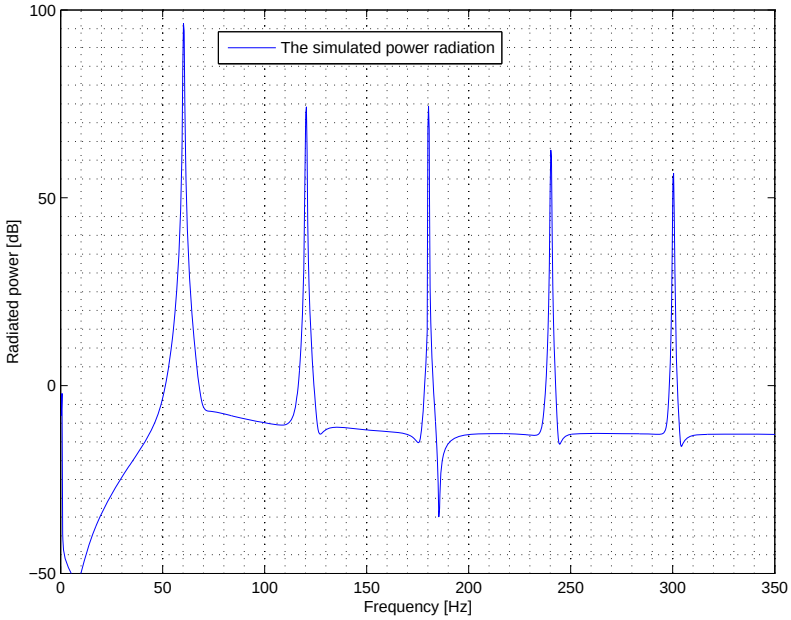

Figure 5.10: *The simulation of the excursion in relative dB, from 0 to 350 Hz.*

CHAPTER 6

Control Scheme for Nonlinearities in the Driver

In chapter 1 on page 15 the basic of the control schemes where describe. The basic of the control scheme, only described how the problem listed could be solved. It did not describe the details of the listed solution. In the chapter it was not possible to set more details due to the little knowledge of the driver. After the model have be derived and analyzed, the controller can be specified.

6.1 Adaptive Control

To design the adaptive control for the driver the following will describe the scheme used. The fundamental scheme is shown in Figure 1.3 on page 16. The control will be designed using the setup shown in Figure 6.1.

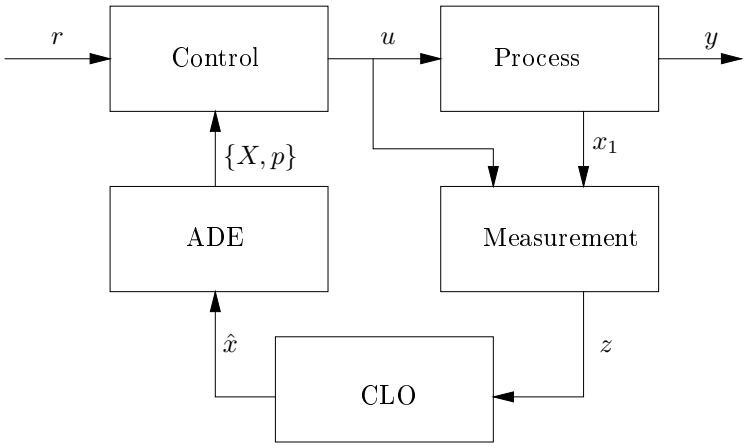

Figure 6.1: *The Adaptive Control Block.*

6.1.1 Measurement Block

The measurement block is used to measure the data needed by the following blocks. It is preferable to measure the excursion, but since this is not possible in the setup, the current used in the driver is measured. The measurement block will have the voltage u and the current i as input.

The measurement block scales the input signals making it possible to load into the computer/DSP. The measurement blocks output are the measurement, z_k.

6.1.2 Closed Loop Observer Block

The Closed Loop Observer (CLO) block is used to observe the non measurable states. From the measurement block the current and voltage is provided. The remaining states are estimated using these information. There is used a KF as observer. The CLO generates an output vector consisting of the states to adaptive estimator block.

6.1.3 Adaptive Estimator Block

In the adaptive estimator block the parameters and states are update on behalf of the information given from the CLO block. These updated parameters and states are used in the controller block.

6.1.4 Controller Block

The controller block comprehends a correction scheme, such that the nonlinearities of the driver can be corrected. The audio signal, r is altered in a way such that this correction is achieved. The corrected signal u is the output. The controller uses a model of the driver with updated states and parameter to calculate the control signal.

CHAPTER 7

Measurement Block

In chapter 6 the control scheme describes the measurement needed in order to compensate for the nonlinearities in the driver. The voltage applied over the driver, and the current supplied to the driver is measured.

7.1 Measurement Devices

The two devices used in the measurement block are

- voltage measurement
- current measurement

The voltage applied over the driver is measured using a voltage divider with a OpAmp mounted as a buffer. The standard voltage divider is set to 1:101. The signal is downscaled in order to measure it with the provided equipment.

The current measurement device used, shall measure the current used in the driver. The current measurement could be done over a resistance, in series with ground, but it would not be precise enough. The resistant should be a very large power resistant, so the temperature and thereby the resistant would not change. B&O provided a device that measures the current running in the cable using a coil. The electrons from the cable flows through the conductor producing a magnetic field. The Hall effect refers to calculating the potential difference on opposite side of an electrical conductor, which is used in the current measuring device (of Standards and Technology, 2007). There will not be enlarged in the function of the measuring device. Using current transducer as current measuring device, does not load the cable and thereby not interfering with the current measurement. This is preferable.

CHAPTER 8

Closed Loop Observer

The closed loop observer, which as to be designed, has been choosen to be of the type KF. This chapter will describe the KF, for understanding the filter, and afterwards a more sophisticated version will be introduced. The closed loop observer, is constructed such that the controller has the necessary information regarding the states. The KF are a type of filter used to estimate the necessary state of a linear system. Since the KF is used on linear systems, and the model made of the driver is a nonlinear system, a other type of KF has been introduced. The other type is the EKF. In the following the general KF will be described, for understanding the filter in general. Afterwards the EKF will be introduced and how it is implemented into the system.

For understanding the use of KF the term filter must be understood. The term filter, is in common a physical device used for removing unwanted elements. But in terms of the KF it resolves into a solution where it includes the measurable states in a system.

The KF is an estimator for solving the problem of estimating the instantaneous state of a linear dynamic system with added white noise. This is done by measuring the states on the linear system. The estimator is statistically optimal with respect to any function of estimation error.

By having this knowledge it is possible to use a KF in many situations where only a limited set of measurements are available to control an object.

8.1 General Kalman Filter

The KF is represented in various type to accomplish different task. In this section the general KF will be describe, and afterwards a description of a KF adapted for the driver model is introduced(Grewal and Andrews, 2001). The dynamical and measurement model used are:

$$x_k = F_{k-1}x_{k-1} + G_{k-1}u_{k-1} + w_k, \qquad w_k \sim \mathcal{N}(0, Q_k) \tag{8.1}$$

$$z_k = H_k x_k + v_k, \qquad v_k \sim \mathcal{N}(0, R_k) \tag{8.2}$$

where F_{k-1} is the dynamical model, G_{k-1} is the control input model, u_{k-1} is the input signal, w_k is the process noise with the normal distribution Q_k where Q_k is the covariance of the process noise. H_k is the measurement sensitivity matrix and v_k is the measurement noise with the normal distribution R_k and R_k is the covariance of the measurement noise.

The optimal linear estimate is equivalent to the general optimal estimator if the variables x and z are jointly Gaussian. Thereby it is preferable to find an update estimate $\hat{x}_k(+)$ based on the observation z_k. The update estimate is a linear function of the prior estimate and the measurement z_k and described as,

$$\hat{x}_k(+) = \hat{x}_k(-) + \overline{K}_k[z_k - H_k\hat{x}_k(-)], \tag{8.3}$$

where $\hat{x}_k(-)$ is the prior estimate of the x_k and $\hat{x}_k(+)$ is the posterior value of the estimate. To get the posterior value of the estimate the Kalman gain $\overline{K}_k$ has to be calculated.

$$\overline{K}_k = P_k(-)H_k^T \left[H_k P_k(-) H_k^T + R_k\right]^{-1} \tag{8.4}$$

where $P_k(-)$ is the error covariance extrapolation

$$P_k(-) = F_{k-1}P_{k-1}(+)F_{k-1}^T + Q_{k-1} \tag{8.5}$$

where $P_k(+)$ is the error covariance update

$$P_k(+) = \left[I - \overline{K}_k H_K\right] P_k(-) \tag{8.6}$$

and F_{k-1} is the dynamical model of the system.

The computational procedure for the discrete KF estimator is as follows (Grewal and Andrews, 2001). First calculate the $P_k(-)$ using the priori values $P_{k-1}(+)$, F_{k-1} and Q_{k-1}. Next compute $\overline{K}_k$ using $P_k(-)$, H_k and R_k. Using $\overline{K}_k$ and $P_k(-)$ the $P_k(+)$ can be computed. Last step is to compute the successive values of $\hat{x}_k(+)$ using $\overline{K}_k$ and given the initial estimate $\hat{x}_0$ and input z_k.

Implementation of the KF is shown in Figure 8.1.

The first block represents the discrete system. The system consists of the real driver, represented with F_{k-1}. There are added process noise w_{k-1} to the states, before they are measured in the next block. The delay box indicates a delay before the next discrete step is preformed. In the measurement block, the measurement matrix H is present. The measurement matrix determines which states are used in the KF to estimate the remaining states. The output is the states which are added with a measurement noise due to the measurement device. The measurement device it assumed not to be perfect. The discrete KF contains a copy of the discrete system shown by the F_{k-1}. This model uses the priori estimated state to calculate the state estimation $\hat{x}_k(-)$. Using the measurement matrix the estimated measurement is calculated and subtracted from the measured value z_k obtaining the error $\tilde{z}_k$. Multiplying the error with $\overline{K}_k$ and adding the state estimate $\hat{x}_k(-)$ the $\hat{x}_k(+)$ is achieved as stated in (8.3).

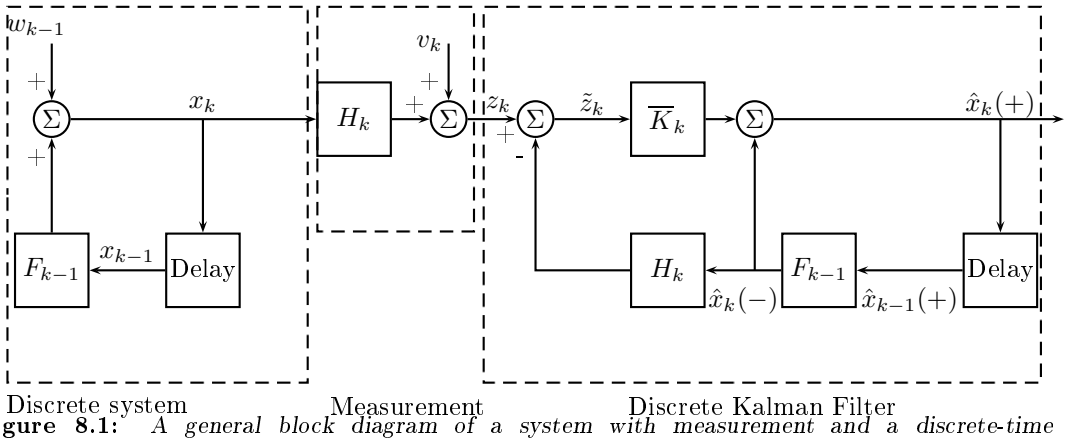

Figure 8.1: *A general block diagram of a system with measurement and a discrete-time KF (Grewal and Andrews, 2001).*

The KF is a good estimator for linear systems, but not for nonlinear system due to the linearization process. It is preferable with a estimator designed for nonlinear systems. This will be introduced in the next section.

8.2 Discrete Extended Kalman Filter

The linearized filtering approach, which is used in the standard KF has a more efficient real-time implementation, but due to its less robustness against nonlinear approximation errors the EKF is preferable.

The EKF improves the KF to estimate nonlinear problems by shaping a Gaussian approximation to the joint distribution of the states and measurements by using a transformation based on a Taylor series.

The EKF works by finding the nominal trajectory. This is done on-line by estimating the current best of the actual trajectory. This approach has the advantage that it only include the state estimation errors, which gives a smaller deviation than any predefined trajectory, as should be used for a linear approximation. The EKF is therefore preferred for this project(Grewal and Andrews, 2001).

The equation used for the discrete EKF are much similar to the KF equations. The nonlinear dynamic model for calculating the state x_k from the previous time step

$$x_k = f_{k-1}(x_{k-1}, u_k) + w_{k-1}, \qquad w_k \sim \mathcal{N}(0, Q_k), \tag{8.7}$$

where w_k is the process noise, with the normal distribution Q_k where Q_k is the covariance of the process noise, and the nonlinear measurement model

$$z_k = h_k(x_k) + v_k, \qquad v_k \sim \mathcal{N}(0, R_k). \tag{8.8}$$

where v_k is the measurement noise with the normal distribution R_k and R_k is the covariance of the measurement noise.

The EKF can, as well as the KF, be divided into two steps,(Grewal and Andrews, 2001)

Prediction:

$$\hat{x}_k(-) = f_{k-1}(\hat{x}_{k-1}(+), u_k) \tag{8.9}$$
$$P_k(-) = F_k P_{k-1}(+) F_k^T + Q_{k-1} \tag{8.10}$$

Update:

$$\hat{z}_k = h_k(\hat{x}_k(-)) \tag{8.11}$$
$$\overline{K}_k = P_k(-) H_k^T \left[H_k P_k(-) H_k^T + R_k \right]^{-1} \tag{8.12}$$
$$\hat{x}_k(+) = \hat{x}_k(-) + \overline{K}_k (z_k - \hat{z}_k) \tag{8.13}$$
$$P_k(+) = \left[I - \overline{K}_k H_k \right] P_k(-), \tag{8.14}$$

where the matrices F_{k-1} and H_k are the Jacobians of f and h

$$F_{k-1} \approx \left. \frac{\partial f_k}{\partial x} \right|_{x=\hat{x}_{k-1}(-)} \qquad H_k \approx \left. \frac{\partial h_k}{\partial x} \right|_{x=\hat{x}_k(-)} \tag{8.15}$$

The dimensions of matrices and vectors in the nonlinear model are presented in Table 8.1.

The difference between the EKF and the KF is the matrices F_k and H_k in the KF are replaced with the Jacobian matrices, (8.15), in the EKF.The disadvantage of the EKF is the added computational cost, due to the calculation of the linearization. The Jacobian matrices need to exist in order to preform the transformation. However these can be a difficult to calculate and can provoke human errors in the derivation or programming. These errors are very hard to debug, because it is hard to determine which part of the estimation produces the error.

The driver where found to be a nonlinear system, and therefore the EKF will be used in this thesis for state estimation. Applying the filter to this project is described in the next section.

Table 8.1: *Dimension of matrices and vectors in the nonlinear model, n is the number of states and l is the number of measurements.*

Symbol	Dimensions
x, f, w	$n \times 1$
Q	$n \times n$
z, h, v	$l \times 1$
R	$l \times l$

8.3 Applying the Extended Kalman Filter

The EKF is chosen for this thesis, and has to be implemented. The implementation follows the equations used in section 8.2 on the preceding page.

The states in the system are as follows:

$$\begin{bmatrix} x_1 \\ x_2 \\ x_3 \end{bmatrix} = \begin{bmatrix} i \\ x_p \\ \dot{x}_p \end{bmatrix}. \tag{8.16}$$

The discrete nonlinear system F is presented in (5.7) on page 36, together with the observation matrix H.

The initial condition for the estimator is chosen to be $\hat{x}_0 = [0\ 0\ 0]^T$. The covariance of the noise is initial chosen to be:

$$Q = \begin{bmatrix} 0.0001 & 0 & 0 \\ 0 & 0.0001 & 0 \\ 0 & 0 & 0.0001 \end{bmatrix} \tag{8.17}$$

$$R = \begin{bmatrix} 0.0001 \end{bmatrix} \tag{8.18}$$

8.4 Verifying the Estimation

The EKF has been applied to the system, to predict the states in the system using only the measurement as input. To verify the filter applied to the system, the filter will be tuned for estimation on a simulated signal, in the linear range and in the nonlinear range of the driver. This is done to verify that the filter can adapt to the system, no matter the systems condition.

Afterwards a test will be performed using measured data from the used driver.

8.4.1 Test Setup

The test is preformed using Matlab. The drivers states are simulated using the `ode45` solver. The solver returns x_1, the current, which are used as the measurement for the EKF along with the voltage, to estimate the remaining states. The input signal is a 10 V_{RMS} 60 Hz sinusoid for tuning of the parameters. The states estimated by the EKF are compared with the simulated driver. After tuning the simulation is preformed with two different signals. A 10 V_{RMS} 60 Hz sinusoid to test the linear range, and a 20 V_{RMS} 60 Hz sinusoid to test the outer range.

The next test will use the data measured at B&O to estimate the states. This estimation will afterward be compared with the measured states, see appendix B for further details.

8.4.2 Result of the Test

The first test with the simulated driver model and the EKF can be seen in Figure 8.2. The figure shows the simulated and estimated states after a tuning of the noise parameters. The final covariance of the noise can be seen in (8.19) and (8.20).These are chosen from analysis of the system. The noise is assumed to be as written. The excursion is more sensitive to noise than the other states, because it operates in a smaller area, therefore this covariance is smaller.

The figure shows the first millisecond of the simulation. The estimation follows the simulation. The difference between the estimated and simulated are small, and the EKF is working properly in the linear range. Figure 8.3 shows the absolute error between the estimated and simulated states. It is expected with some kind of error, since the simulated states are added with a noise. But the deviation caused by the error is small, and does not effect the estimation.

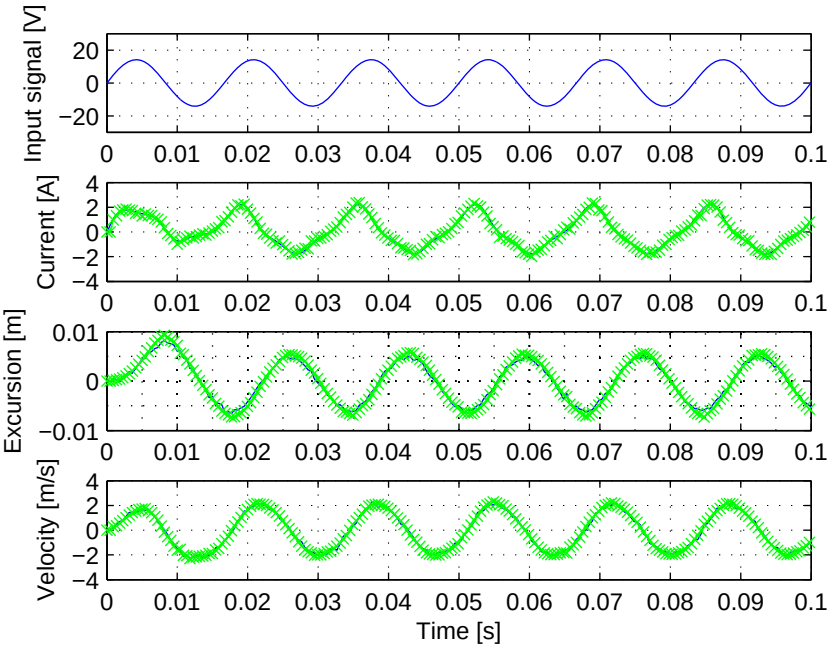

Figure 8.2: *The simulated (-) and estimated (-x) states after tuning the parameters.*

$$Q = \begin{bmatrix} 0.01 & 0 & 0 \\ 0 & 10^{-6} & 0 \\ 0 & 0 & 0.01 \end{bmatrix} \tag{8.19}$$

$$R = \begin{bmatrix} 0.01 \end{bmatrix} \tag{8.20}$$

Testing the estimator in the nonlinear range gives the result shown in Figure 8.4. The Figure clearly show the driver is in the nonlinear range. The excursion is only moving in the positive range, and the current is limited when moving in the positive range. The error of can be seen in Figure 8.5. The estimation works properly and estimates the states even when the driver is operating in the nonlinear range.

The next test is preformed on measured data made at B&O. The voltage, current and excursion where measured during a test preformed on the used driver. The input is a 10 V_{RMS} 60 Hz sinusoid. The output of the estimator is shown in Figure 8.6. As mentioned in appendix B the current measurement has a small error, which also is shown in the Figure. This effects the

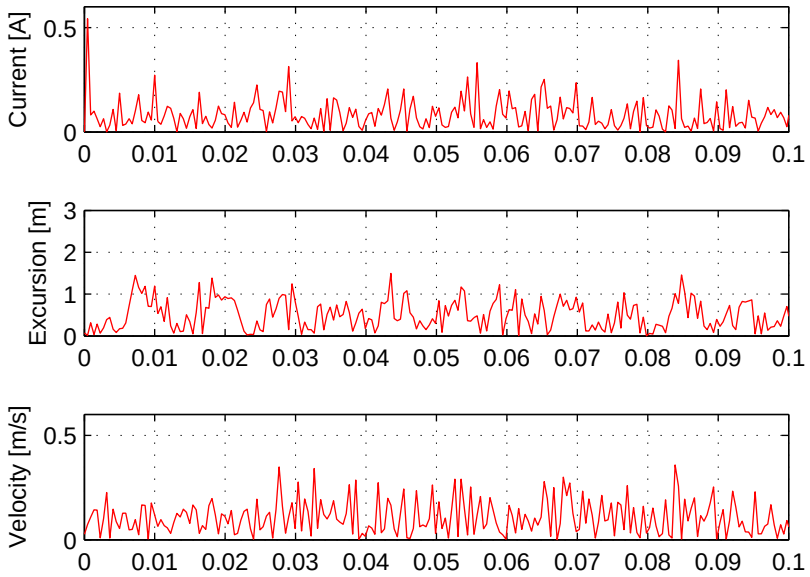

Figure 8.3: *The absolute error of the estimated and simulated states.*

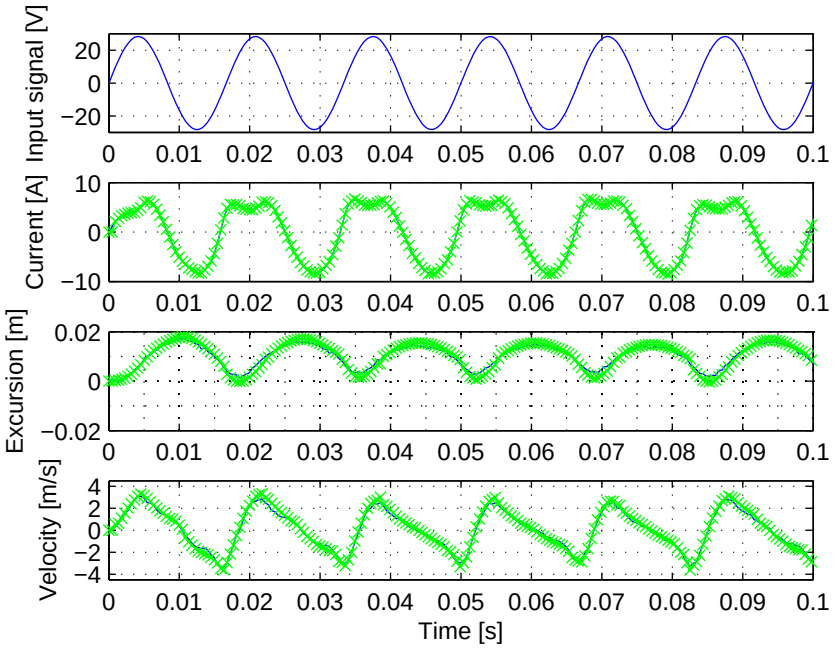

Figure 8.4: *Estimation in the nonlinear range, simulated (-) and estimated (-x) states.*

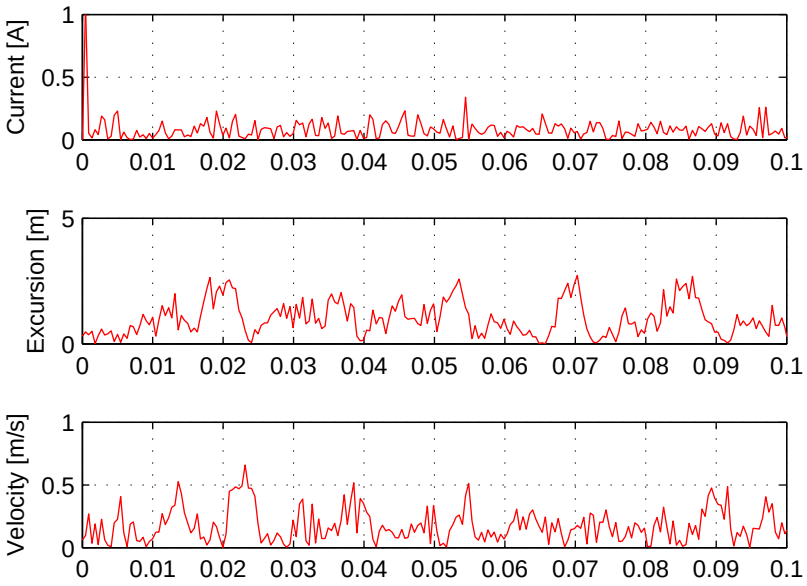

Figure 8.5: *The absolute error of the estimated and simulated states in the nonlinear range.*

estimator since the current is the input. The estimation of the excursion has a larger error at the same point in each period, which can be seen in Figure 8.7, this is because of the error in the current measurement. This also relates to the velocity estimation. The velocity was not measured and is therefor zero.

8.5 Summery

This chapter has introduced the general KF and the discrete EKF. The EKF has been implemented into this project because of its better function regarding nonlinear systems. The parameter of the filter is tuned and used in a simulation of the EKF and the driver. The results showed that the EKF could estimate the states of the driver in the linear and nonlinear range. The estimator was also tested on real measured states, from a test made at B&O. Because of an error in the current measurement, the comparison of the states had some error. This is because the current measurement is used in the EKF which estimates a wrong excursion, when compared to the real excursion measurement.

Over all the EKF function correct, and it is possible to estimate the excursion and velocity using the current and input voltage.

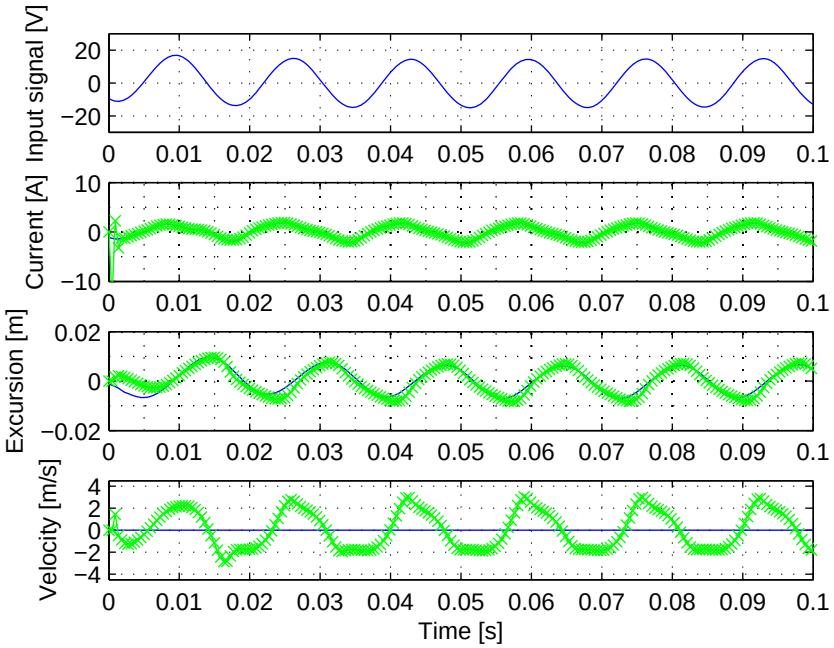

Figure 8.6: *An estimation preformed on a real measurements, measurement (-) estimation (-x).*

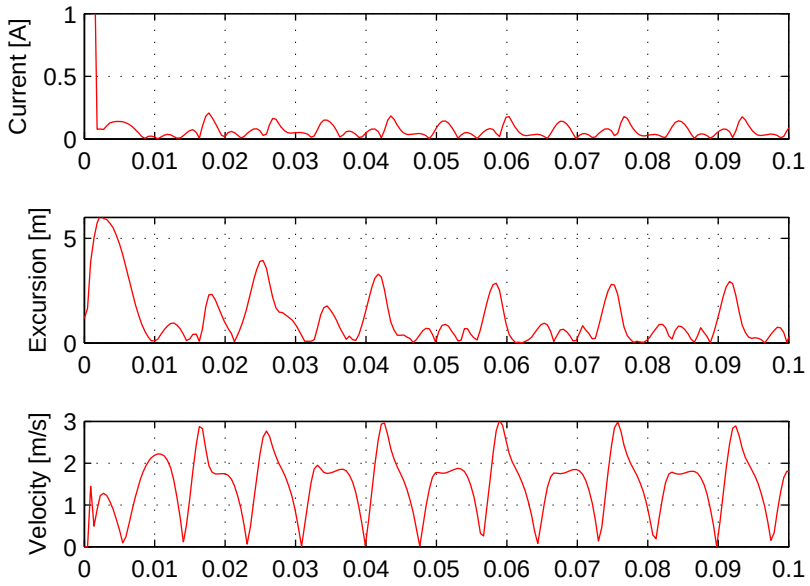

Figure 8.7: *The absolute error between the measured and simulated states.*

CHAPTER 9

Nonlinear Control

In order to reduce the harmonic distortion in the driver a control framework has to be developed. The framework which will be presented in this chapter is a nonlinear control law added to the system. After the nonlinear control law is added, a linear controller will be adjusted to the system such that the desired behavior is archived.

The nonlinear control framework is the well known feedback linearization control. This type of control scheme has been used for many years in different control applications.

9.1 Feedback Linearization

The framework, feedback linearization, is an approach in which a nonlinear system is transferred into an equivalent linear system. The nonlinear controller are designed by first determining the influence of u on y, and afterwards transform the nonlinear system into a linear system by using the diffeomorphism. The feedback linearization scheme is design on basis of(Khalil, 2002).

In Figure 9.1 the overall framework of the nonlinear control law is shown.

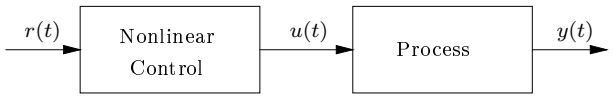

Figure 9.1: *Nonlinear Control framework.*

The nonlinear system is on the form

$$\begin{aligned} \dot{x} &= f(x) + g(x)u \\ y &= h(x) \end{aligned} \tag{9.1}$$

with $f(0) = 0$.

9.2 Input-State Linearization

In order to apply the control law of the nonlinear system, the control law used are made in two steps.

1. Transform the nonlinear system into an integrator decoupled system by a nonlinear static state feedback.
2. The desired linear dynamics are applied.

This framework is shown in Figure 9.2.

Figure 9.2: *The nonlinear control in two step.*

The linearizing diffeomrphism for a SISO system represented by (9.1) is given by

$$\xi = T(x) = \begin{bmatrix} h(x) \\ L_f h(x) + L_g h(x) u \\ L_f^2 h(x) + L_g L_f h(x) u \\ \vdots \\ L_f^d h(x) + L_g L_f^{d-1} h(x) u \end{bmatrix} \tag{9.2}$$

The nonlinear static state linearizing state feedback is given by

$$u = -\alpha(x) + \beta(x) v = -\frac{L_f^d h(x)}{L_g L_f^{d-1} h(x)} + \frac{1}{L_g L_f^{d-1} h(x)} v \tag{9.3}$$

By applying the feedback control to the system the linear and nonlinear dynamics of the system is canceled due to the inversion. The input v of the inverse dynamics is after the applied control law an integrator decoupled system of order d,

$$y^{(d)} = v. \tag{9.4}$$

This can in state space form be represented by the Brunovski canonical form

$$\dot{\xi} = \begin{bmatrix} 0 & 1 & 0 \\ & \ddots & \vdots \\ & & 1 \\ 0 & 0 & 0 \end{bmatrix} \xi + \begin{bmatrix} 0 \\ \vdots \\ 0 \\ 1 \end{bmatrix} v. \tag{9.5}$$

or in normal form

$$\dot{\xi} = A_C \xi + B_C v. \tag{9.6}$$

The final step in making the feedback linearization controller for the driver is obtaining the linear dynamic of the system, which reduces the harmonic distortion. To obtain this condition the poles of the decoupled system should be placed so the desired linear behaviour is fulfilled.

9.3 Determining the Relative Degree

As described the output, y does not depend explicitly on u since u is not an argument of function $h(x)$. If u is changed instantaneously, there will not be an immediate change of y, the change comes gradually via x.

To determine the influence of u on y the relative degree must be determined.

According to definition the system given by (9.1) has relative degree d at a point x_0 if

1. $L_g L_f^{k-1} h(x) = 0$ for all x in a neighbourhood of x_0, $k = 1, \ldots, d-2$ and
2. $L_g L_f^{d-1} h(x_0) \neq 0$.

where $L_f h(x)$ is Lie derivative of $h(x)$.

The relative degree d for the system is obtained by the following calculations

$$\frac{d^k y}{dt^k} = y^{(k)} = \begin{cases} L_f^k h(x), & k = 1, \ldots, d-1 \\ L_f^k h(x) + L_g L_f^{k-1} h(x) u, & k = d \end{cases} \tag{9.7}$$

Hence the output represent the excursion of the diaphragm, x_2. The relative degree equals the number of state, $d = n$. Since $d = n$, zero dynamics does not need to be taken into consideration.

The calculations of the relative degree for the system yields $d = 3$.

9.4 Linearization of the system

After the algorithm for the linearization feedback control has be described the algorithm is used on the system (9.1). In order to apply the control law, the diffeomorphism has to be known. The diffeomorphism yields,

$$\begin{aligned} \xi_1 &= h(x) = x_2 \\ \xi_2 &= L_f h(x) + L_g h(x) u = x_3 \\ \xi_3 &= L_f^2 h(x) + L_g L_f h(x) u = \left(\tfrac{Bl(x_2)}{M_D} + \tfrac{L_{ex}(x_2) x_1}{2 M_D} \right) x_1 - \tfrac{k(x_2)}{M_D} x_2 - \tfrac{R_m}{M_D} x_3 \end{aligned} \tag{9.8}$$

By applying the coordinate transformation (9.8) and use the information on (9.3) yields the control law to obtain the feedback linearization of the driver

$$\begin{aligned} u = & \frac{L_e(x_2)}{Bl(x_2) + L_{ex}(x_2) x_1} \left(x_3 \left[k_x(x_2) x_2 + k(x_2) - Bl_x(x_2) x_1 - \frac{R_m^2}{M_D} - \frac{L_{exx}(x_2)}{2} x_1^2 \right] \right. \\ & \left. - \frac{R_m k(x_2)}{M_D} x_2 + \frac{R_m x_1}{M_D} \left[Bl(x_2) + L_{ex}(x_2) \frac{x_1}{2} \right] \right) + R_e x_1 + Bl(x_2) x_3 + L_{ex}(x_2) x_1 x_3 \\ & + \frac{L_e(x_2) M_D}{Bl(x_2) + L_{ex}(x_2)} v. \end{aligned} \tag{9.9}$$

The control law applied to the system yields an integrator decoupled system given by $y^d = v = \dot{\xi}_3$, meaning that the output of the transformed system is located from $y = \int\int\int \dot{\xi}_3 dt dt dt = \xi_1 = x_2$, which is also the output of the original system.

9.5 Design of Compensator

The desired linear dynamical behavior of the system is found by use of pole placement on the transformed system given by (9.5).

$$\dot{\xi} = \begin{bmatrix} 0 & 1 & 0 \\ 0 & 0 & 1 \\ -\lambda_0 & -\lambda_1 & -\lambda_2 \end{bmatrix} \xi + \begin{bmatrix} 0 \\ 0 \\ \lambda_3 \end{bmatrix} r. \tag{9.10}$$

The (9.10) is the controller canonical form having the desired canonical polynomial that equals the desired linear system matrix A. In section 5.6 the system is found to be observable, and hence the rank of observable matrix of A is equal the numbers of the states the stability of the closed loop is guaranteed.

The desired linear dynamical behavior for the system is found from the characteristic polynomial of A (all the nonlinear parameters set to zero). Together with (9.10) results in a linear state space model given by

$$\begin{bmatrix} \dot{\xi}_1 \\ \dot{\xi}_2 \\ \dot{\xi}_3 \end{bmatrix} = \begin{bmatrix} 0 & 1 & 0 \\ 0 & 0 & 1 \\ -\frac{R_e k_0}{M_D L_{e0}} & -\left(\frac{R_e R_m}{M_D L_{e0}} + \frac{k_0}{M_D} + \frac{Bl_0^2}{M_D L_{e0}}\right) & -\left(\frac{R_e}{L_{e0}} + \frac{R_m}{M_D}\right) \end{bmatrix} \begin{bmatrix} \xi_1 \\ \xi_2 \\ \xi_3 \end{bmatrix} + \begin{bmatrix} 0 \\ 0 \\ \frac{Bl_0}{M_D L_{e0}} \end{bmatrix} r. \tag{9.11}$$

The compensator is design by using the result found in (9.8) and combining it with the equation for the compensator given by

$$v = -\sum_{i=0}^{n-1} \lambda_i y^{(i)} + \lambda_n r \tag{9.12}$$

$$v = -\lambda_2 \left(\frac{Bl(x_2)}{M_D} + \frac{L_{ex}(x_2)x_1}{2M_D}\right) x_1 + \left(\frac{\lambda_2 k(x_2)}{M_D} - \lambda_0\right) x_2 + \left(\frac{\lambda_2 R_m}{M_D} - \lambda_1\right) x_3 + \lambda_3 r. \tag{9.13}$$

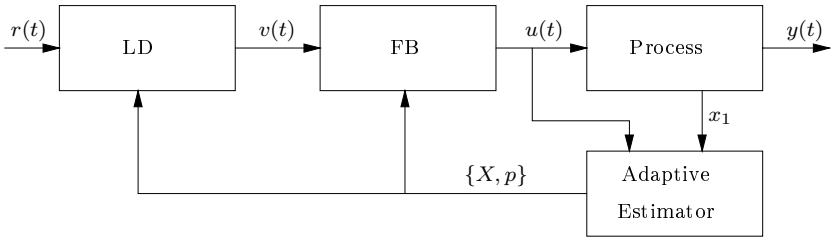

Figure 9.3: *The nonlinear controller added to the system, by use of the feedback linearization control law.*

To deploy the nonlinear controller, shown in Figure 9.3 full state information has to be reached. By use of the information of the acceleration, $\dot{x}_3$ the inverse dynamic control compensator (9.9) can be simplified to

$$u = \frac{L_e(x_2)}{Bl(x_2) + L_{ex}(x_2)x_1} \left(x_3 \left[k_x(x_2)x_2 + k(x_2) - Bl_x(x_2)x_1 - \frac{L_{exx}(x_2)}{2} x_1^2\right] + R_m \dot{x}_3\right)$$
$$+ R_e x_1 + \left(Bl(x_2) + L_{ex}(x_2)x_1\right) x_3 + \frac{L_e(x_2) M_D}{Bl(x_2) + L_{ex}(x_2)x_1} v. \tag{9.14}$$

Since information on the acceleration is available using this information is preferable in the nonlinear compensator. The linear dynamic parts (9.13) are also simplified by use of the acceleration,

$$v = \lambda_0 x_2 - \lambda_1 x_3 - \lambda_2 \dot{x}_3 + \lambda_3 r. \tag{9.15}$$

By combining the compensator of the linear dynamic and the nonlinear part, further simplification is achievable. To avoid the linear terms, which is subtracted in the nonlinear part, are added again, in the linear part a substitution is made. The substitution results in one input-output description of the linearization compensator

$$\begin{aligned} u = & \frac{L_e(x_2)}{Bl(x_2) + L_{ex}(x_2)x_1} \left[\left(k_x(x_2)x_2 + (k(x_2) - k_0) - Bl_x(x_2)x_2 - \frac{L_{exx}(x_2)}{2} x_1^2 - \frac{Bl_0^2}{L_{e0}} \right) x_3 \right. \\ & \left. + \frac{R_e\,(k(x_2) - k_0)}{L_{e0}} x_2 - \frac{R_e\,(2Bl(x_2) + L_{ex}(x_2)x_1)}{2L_{e0}} x_1 \right] + R_e x_1 + Bl(x_2)x_3 + L_{ex}(x_2)x_1 x_3 \\ & + \frac{L_e(x_2)Bl_0}{Bl(x_2) + L_{ex}(x_2)x_1 L_{e0}} r. \end{aligned} \tag{9.16}$$

The compensator requires full state information in order to compensator the nonlinearity in the driver. The simplification of the compensator shows that the knowledge of the mass is not needed, either is the resistance of the mechanical part.

9.6 Simulation of Compensator

The compensator has been designed and a simulation will determine the performance of the designed compensator. The compensator is design such that the harmonics in the driver will be reduced, due to the placement of the poles.

The simulation of the non-compensated system and the compensated system is shown in the following figures. The simulation is made by analysing the radiated power of the excursion in dB, by use of the FFT analysis method, such that the harmonic tones and the reduction is shown. In chapter 4 the method of calculating the radiated power is described.

The generated input signal r is sinusoid with a 60 Hz frequency, sampled in 3 seconds with a sampling frequency fs of 44.1 kHz, and an amplitude of 10 V_{RMS}.

$$\begin{aligned} r &= A\sin(2\pi \cdot fs \cdot t \cdot Hz) \\ &= 10\sqrt{2}\sin(2\pi \cdot 44100 \cdot 3 \cdot 60) \end{aligned}$$

The harmonics generated in the driver are shown in Figure 9.4, where the result of the compensator is shown as well. The reductions of the harmonics are shown in Table 9.1.

Inspecting the figure, and the table, shows that the compensator does not abate the harmonics as expected. The harmonics are abated with 80% or more, except the 3. harmonic which is only abated with 66%. The compensator is chosen to be used in the further work.

By increasing the sampling frequency the update of the parameter and the states is increased, and the compensator correction of the input signal is also optimised. By increasing the sampling frequency with a factor 2 the sampling frequency is set to 88.2 kHz. In Figure 9.5 the result of the increased sampling frequency is shown. It show that the compensator abate the harmonic distortion as expected. No further analysed will be made.

Increasing by a factor 2 is found to be a significant change and found able to compensate for the nonlinear parameters as expected. With use of a sampling frequency of 48 kHz the compensator abates the harmonics. The third harmonic is not abated as expected. The result of setting the sampling frequency at 48 kHz is found to be preferable, as shown in Figure 9.6.

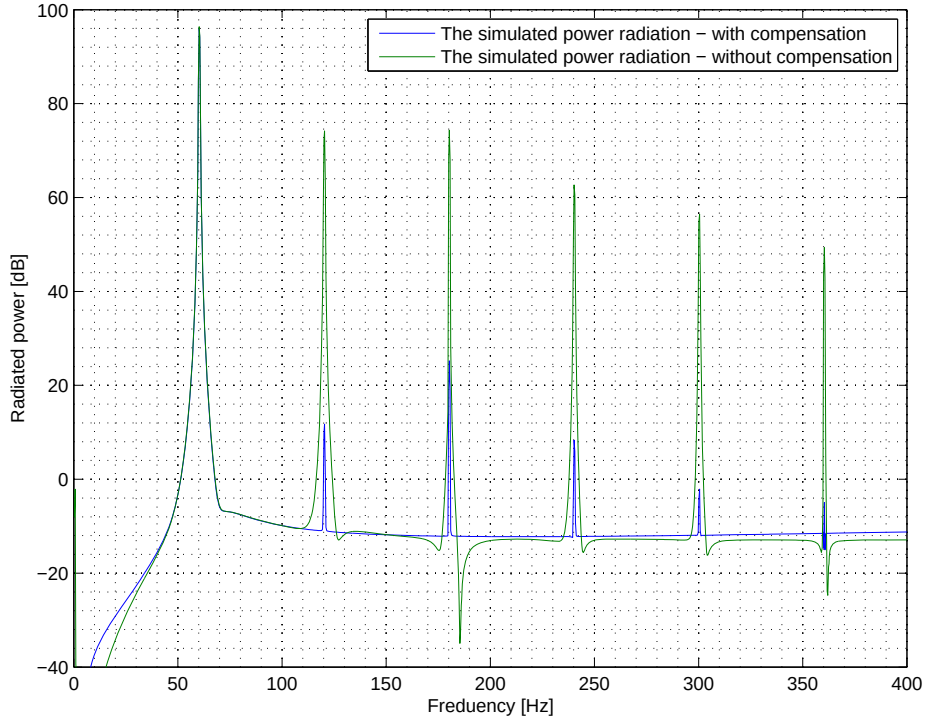

Figure 9.4: *The simulation of the excursion with and without the compensator. The signal used is an sinusoid 10* V_{RMS} *at 60 Hz.*

Harmonic	Without Compensator	With Compensator	Reduction
2.	74 dB	9 dB	84%
3.	74 dB	25 dB	66%
4.	62 dB	8 dB	87%
5.	56 dB	−2 dB	103%
6.	49 dB	−5 dB	110%

Table 9.1: *The diffenrence of the harmonics due to the compensator.*

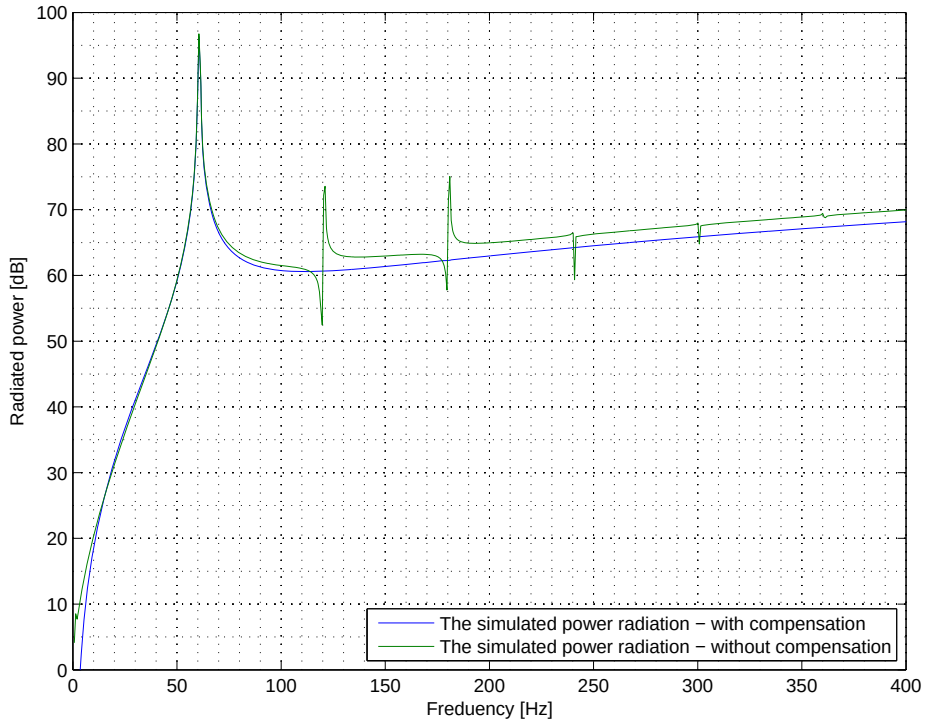

Figure 9.5: *The radiated power of the excursion, at an increased sampling frequency of a factor 2.*

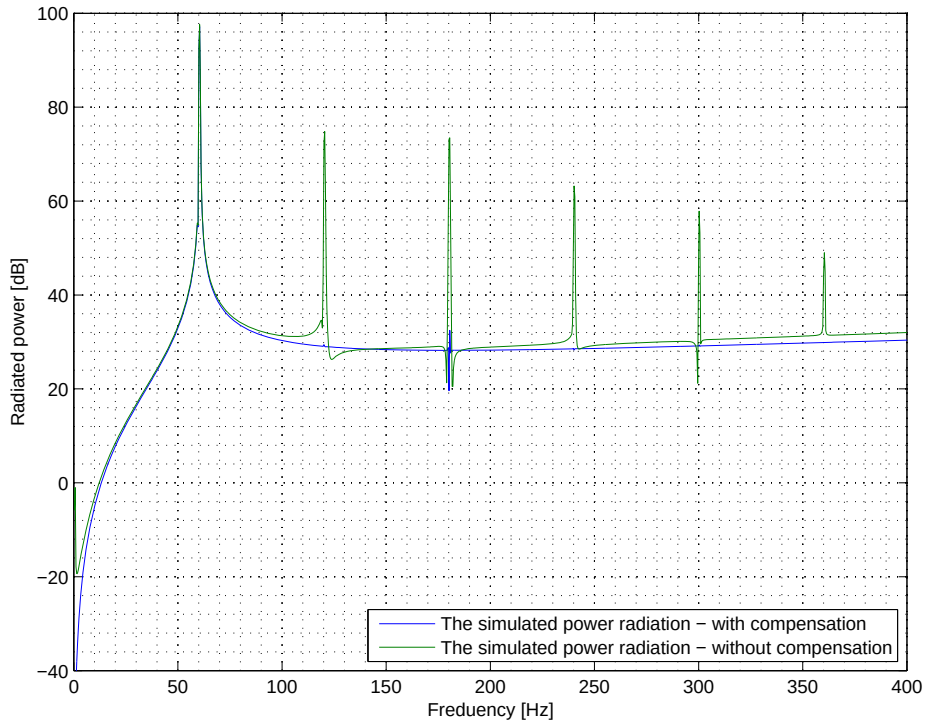

Figure 9.6: *The radiated power of the excursion, with* $fs = 48$ *kHz.*

CHAPTER 10

System Identification

The system identification is designed such that the control block have the information regarding the states and the parameters that are necessary for the correction part.

Designing the adaptive estimation block can be done in several ways, depending on the information available for the block and what information shall be used later in the process. As shown on Figure 6.1 the control block needs information regarding the states, therefore a model of the driver can be used. Also since a CLO is used to determine the states.available, this solution seems preferable leaving out the model of the driver. One can also combine the two, using the Filter information and the information from the model and use them in combination. By using them in a combination an error of the states can be used to calculate the parameters - described later. In this thesis only the filter information is used.

Identifying the parameters such that the change due to time, temperature and age etc. are detected, can been made using different algorithms.

10.1 Parameter Update using MSE

The parameters which are depending on the excursion of the voice coil can be identified and updated using a cost function as the Mean Square Error (MSE).

$$MSE = J = E\left[(e(i))^2\right] \tag{10.1}$$

They can be determined by the Adaptive Estimator by searching for the minimum of the cost function, where the partial derivatives of the cost function in respect to the parameters who are to be determined become zero. The algorithm can be processed by an iterative calculation - Least-Mean Square (LMS) algorithm. In section 3.1 the parameters who needs to be identified are approximated with a fourth order polynomial. The coefficients for the polynomial can be updated as follows

- Force Factor

$$bl_j(k+1) = b_j(k) + \mu e \frac{\partial e}{\partial bl_j} \tag{10.2}$$

- Stiffness
$$k_j(k+1) = k_j(k) + \mu e \frac{\partial e}{\partial k_j} \tag{10.3}$$
- Inductance
$$l_{ej}(k+1) = l_{ej}(k) + \mu e \frac{\partial e}{\partial l_{ej}}, \tag{10.4}$$

where the coefficients are updated by adding the product of the error signal and the partial derivatives of the error in respect to the coefficient scaled by a learning factor μ.

The error signal for updating the coefficients are calculated by using the fundamental equations (2.2b) and (2.2c), to obtain the error on the velocity.

$$e = \left.\frac{dx}{dt}\right|_{(2.2\text{b})} - \left.\frac{dx}{dt}\right|_{(2.2\text{c})} \tag{10.5}$$
$$= \left(u - R_e i + \frac{d\left(Le(x)i\right)}{dt}\right)\frac{1}{Bl(x)} - \frac{1}{R_e}\left(M_D\frac{d^2x}{dt^2} + k(x)x - \frac{L_x i^2}{2} - Bl(x)i\right) \tag{10.6}$$

The partial derivatives of the error with respect to the coefficients are calculated as

- Force Factor
$$\frac{\partial e}{\partial bl_i} = -\frac{x^i}{Bl(x)^2}\left(R_e i + \frac{d\left(Li\right)}{dt} - u\right) - \frac{x^i i}{R_m} \tag{10.7}$$
- Stiffness
$$\frac{\partial e}{\partial k_i} = \frac{1}{Rm}x^{i+1} \tag{10.8}$$
- Inductance
$$\frac{\partial e}{\partial l_{ej}} = \frac{d\left(x^j i\right)}{dt}\frac{1}{Bl} - \frac{1}{R_m}\frac{j x^{j-1} i^2}{2bl_0} \tag{10.9}$$

10.2 Parameter Update using SVD

For updating and identifying the coefficients of the excursion depended parameters the use of the Singular Value Decomposition (SVD) algorithm can be used. As described in section 3.1 the parameters are modeled as a fourth order polynomial. These coefficients can be updated by use of the SVD.

By use of the SVD algorithm a set of coefficients has to be known, where the each column represents a set of coefficients for a specific driver,

$$\Gamma = \begin{bmatrix} \gamma_{1,1} & \gamma_{1,2} & \cdots & \gamma_{1,n} \\ \gamma_{2,1} & \gamma_{2,2} & \cdots & \gamma_{2,n} \\ \vdots & \vdots & \ddots & \vdots \\ \gamma_{m,1} & \gamma_{m,2} & \cdots & \gamma_{m,n} \end{bmatrix}. \tag{10.10}$$

Calculating the mean of the Γ, gives a representation of the overall driver, Δ

$$\Delta = \begin{bmatrix} \delta_1 \\ \delta_2 \\ \vdots \\ \delta_m \end{bmatrix}, \qquad \text{where} \quad \delta = \frac{1}{n}\sum_{m=1}^{n}\gamma_{m,n} \tag{10.11}$$

Using Δ to obtain the variance Ψ of the Γ by subtracting it

$$\Psi = \begin{bmatrix} \gamma_{1,1} - \delta_1 & \gamma_{2,1} - \delta_1 & \cdots & \gamma_{1,n} - \delta_1 \\ \gamma_{2,1} - \delta_2 & \gamma_{2,2} - \delta_2 & \cdots & \gamma_{2,n} - \delta_2 \\ \vdots & \vdots & \ddots & \vdots \\ \gamma_{m,1} - \delta_m & \gamma_{m,2} - \delta_m & \cdots & \gamma_{m,n} - \delta_m \end{bmatrix}. \tag{10.12}$$

Using the SVD algorithm on the meaned matrix Ψ results in the factorization form

$$U\Sigma V^T = \text{svd}\,(\Psi) \tag{10.13}$$

where U is the unitary matrix, $m \times m$. It contains a set of orthonormal "output" basis vector directions for Ψ. The matrix V^T denotes the conjugated transpose of V. The matrix V thus contains a set of orthonormal "input" basis vector directions for Ψ. The matrix Σ is $m \times n$ with nonnegative numbers on the diagonal (as defined for a rectangular matrix) and zeros off the diagonal. It contains the singular values, which can be thought of as scalar "gain controls" by which each corresponding input is multiplied to give a corresponding output.

The singular values should be identified in the filter block, thereby less computation is needed and often only a few singular values needs to be determined to update all the coefficients.

The new determined singular values Σ^* are used to update the coefficients of the parameter by using the following algorithm

$$\Psi^* = U\Sigma^* V^T \tag{10.14}$$

$$e_{\text{SVD}} = \Psi^* - \Psi \tag{10.15}$$

$$e_{\text{SVD}} \leq T_h \tag{10.16}$$

$$\Gamma^* = \Psi^* + \Delta \tag{10.17}$$

where the Ψ^* are calculated and compare with the old value. Then its compared against a set threshold value T_h. Calculate the Γ^* vector containing the identified coefficients of the parameter.

To use the SVD algorithm for identifying the parameter, a set of coefficients for different drivers must be known. The larger the set can be the more accurate the coefficients will bee. For using this method the drivers coefficients must be of the same type, woofer, tweeter etc. If its possible to group the types, such that the coefficients does have a small variance it is preferable.

10.3 Parameter Update using Kalman Filter

Described earlier the KF can be used to determine the states for a given system. The benefit of such use can also be adapted for use in parameter identification. In normal use the process of determining a nonlinear mapping

$$y_k = G(u_k, p) \tag{10.18}$$

where u_k is the input, y_k is the output, G is the nonlinear map, parametrized by the vector p. The target is to estimate the parameters p. Typical, a set to be evaluated in order to estimate the parameters is provided with a sample of a pair, consisting of a known input and desired output $\{u_k, o_k\}$. The error of the filter is defined as

$$e_k = o_k - G(u_k, p) \tag{10.19}$$

where the main target is to estimate the parameter vector p by use of minimizing the expected squared error.

To estimate and identify the parameter the EKF can be used. For using the EKF to estimate the parameter vector p an new state-space representation is made

$$p_k = p_{k-1} + w_k \tag{10.20}$$
$$y_k = G(u_k, p_k) + e_k \tag{10.21}$$

where the parameters p_k corresponds to a stationary process with identity state transition matrix, driven by the process noise w_k. The output y_k corresponds to a nonlinear observation on p_k. The EKF can thereby be applied directly as an efficient "second-order" technique for estimate the parameters.

By use of this approach two EKF can run simultaneously to estimate the states and the parameters. For every estimation loop, the current estimate of the state is used in the parameter estimation and the current estimate of the parameters are used in the state estimate. The advantaged of running two EKF is that the change of parameters is not as large as the change of the states. Thereby the two filters does not need to have the same sampling frequency, making the computation less demanding. The state and the parameter vector can be combined into a single, joint state vector $[x_k^T w_k^T]^T$. The estimation is done recursively by rewriting the state-space equations

$$\begin{bmatrix} x_k \\ p_k \end{bmatrix} = \begin{bmatrix} F\left(x_{k-1}, p_{k-1}\right) \\ I \cdot p_{k-1} \end{bmatrix} + \begin{bmatrix} B \cdot v_k \\ u_k \end{bmatrix} \tag{10.22}$$
$$y_k = \begin{bmatrix} 1 & 0 & \cdots & 0 \end{bmatrix} \begin{bmatrix} x_k \\ p_k \end{bmatrix} + w_k \tag{10.23}$$

which produces a simultaneous estimation of the states x_k and the parameters p.

CHAPTER 11

Result of Compensation of Driver

The CLO block has been designed and shown that the states of the system can be detected, and the control block has also been designed and verified in such a way that the nonlinearities of the driver is faded out. The overall system in combination is to be proved to work in this chapter. The verification of the overall system is made by combining the three blocks as described in section 6.

11.1 Method of Testing the System

To verify that the compensator works as described, a method of testing the control scheme is to be designed. The method to test the control schemed is to run the simulation with the compensator such that the audio signal is changed in the way needed in order to compensate for the nonlinearities in the driver, and afterwards use the CLO to estimate the states of the system. The estimated states are used in the adaptive estimator block and in the Controller.Run the simulation of a given period of time, and evaluate the result by analysing the radiated power of the excursion with and without the control scheme implemented.

11.2 Expected Validation

The validation of the control scheme must show that the compensator can cancel the nonlinearities such that the drivers performs as a linear device even if the driver is driven in the nonlinear range. Even if there is some small estimation error, according to the description in section 8.4.2 it may not affect the compensator in such a way that it can not perform as expected. The radiated power of the excursion must not show any harmonics in the use of the control scheme and the excursion must be a scale of the audio signal applied to the system. The simulation of the driver in the nonlinear range without control, must show some harmonics and some other disturbances according to its physical limits and modeling of the parameters.

11.3 Result of Simulation

As described, the simulation of the driver should be performed in the nonlinear range. But this was not possible. The calibration of the covariance noise is done in the linear range with 10 V_{RMS} as a 60 Hz sinusoid.

In Figure 11.2 the full test is shown with the compensator and state estimation. The covariance noise has been fitted making the compensator work best. The final noise covariances are:

$$Q = \begin{bmatrix} 1_E - 6 & 0 & 0 \\ 0 & 1_E - 12 & 0 \\ 0 & 0 & 1_E - 6 \end{bmatrix} \quad (11.1)$$

$$R = \begin{bmatrix} 1_E - 1 \end{bmatrix} \quad (11.2)$$

Figure 11.1 shows the input voltage to the driver with and without the compensator.

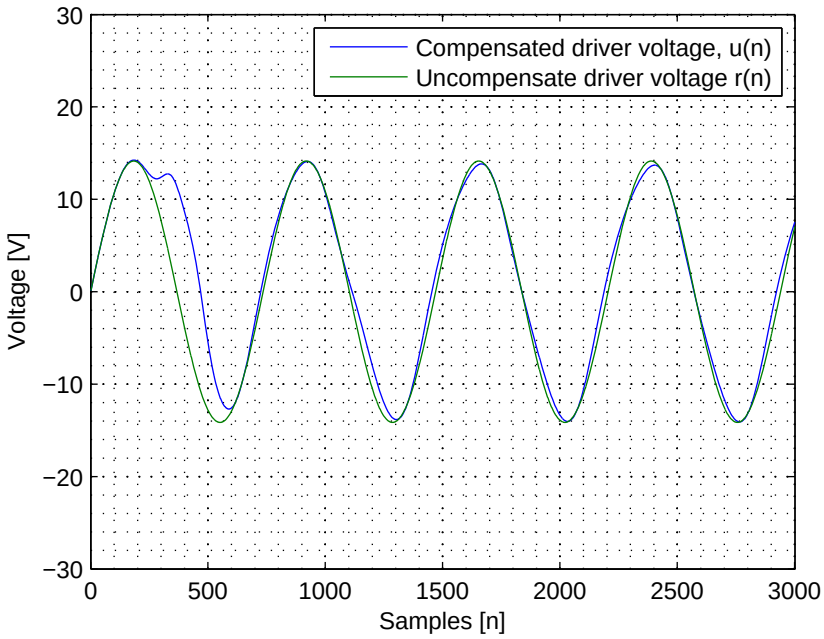

Figure 11.1: *Simulation showing the excursion in linear range.*

The third harmonic is the most dominating harmonic. The amplitude of the third harmonic without compensator is 64.98 dB and with compensator 28.45 dB. This is a significant improvement of 36.53 dB.

A reason for the error in the nonlinear simulation is seen in the beginning of the simulation. Figure 11.3 shows a simulation with an amplitude of 12 V. The compensated signal has a settling time in the first 600 samples. With a larger input signal this deviation could exceed the range of the driver, and thereby creating an error in the simulation.

Implementing a fix in the Matlab script, neglecting the input voltage the first 600 sample, improves the nonlinear simulation. It is possible to simulate with a input voltage of 18 V_{RMS} which is considered in the nonlinear range, also shown in Figure 11.4. The large deviation at sample 1145 reaches -140 V, this appeared in every simulation, but for some reason this did not effect the excursion. The excursion of the compensator shown in Figure 11.5 is without deviation.

The FFT analysis in the nonlinear range is shown in Figure 11.6. The compensator reduces the nonlinearities in the driver, but do not remove them. There is an improvement on the third harmonic on 34.14 dB.

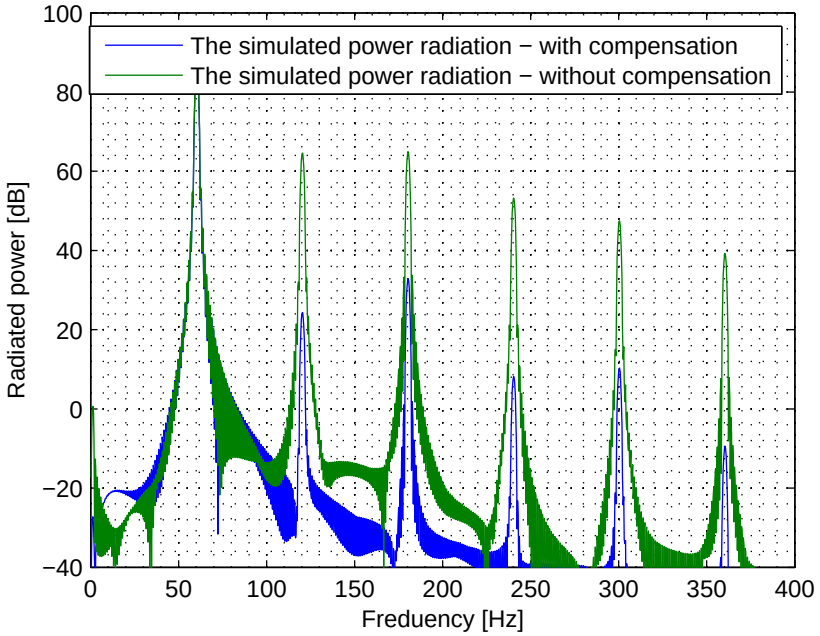

Figure 11.2: *Simulation of driver with state estimation and compensator in the linear range.*

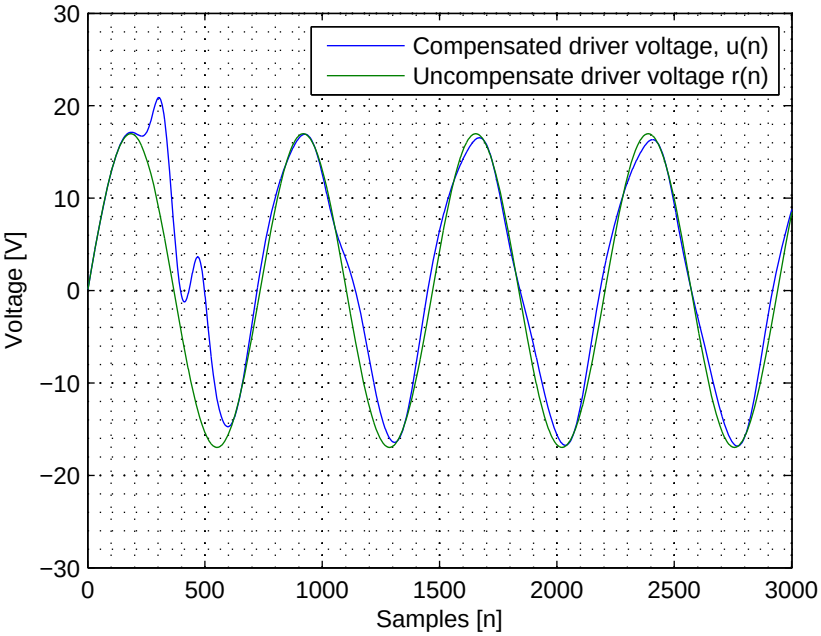

Figure 11.3: *Simulation of system showing deviation in the compensator.*

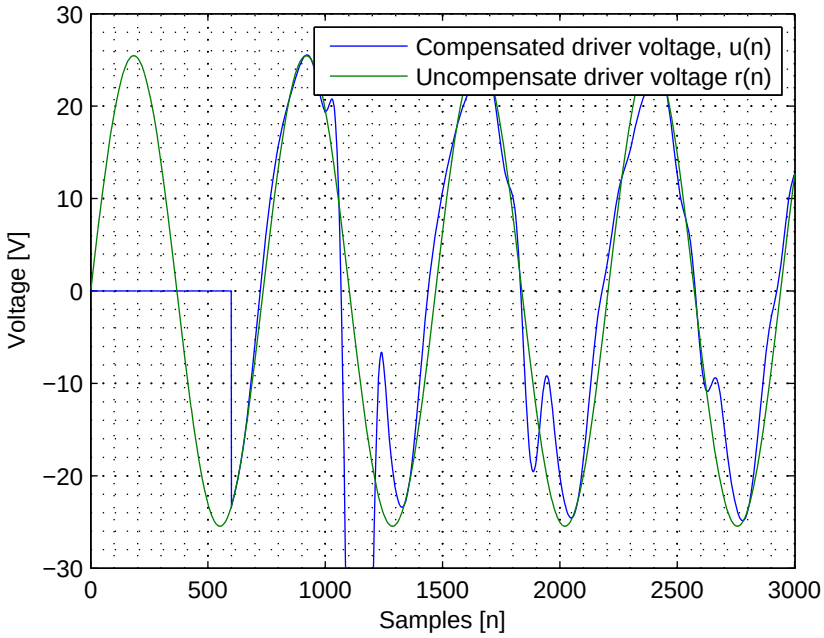

Figure 11.4: *Simulation of system showing nonlinear deviation in the compensator driver voltage.*

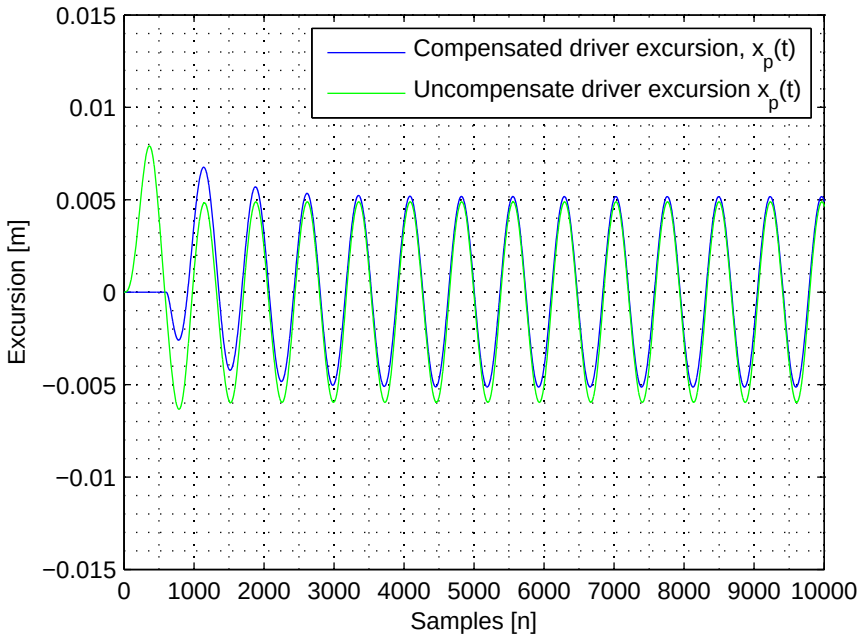

Figure 11.5: *Excursion of simulation of driver with state estimation and compensator in the nonlinear range.*

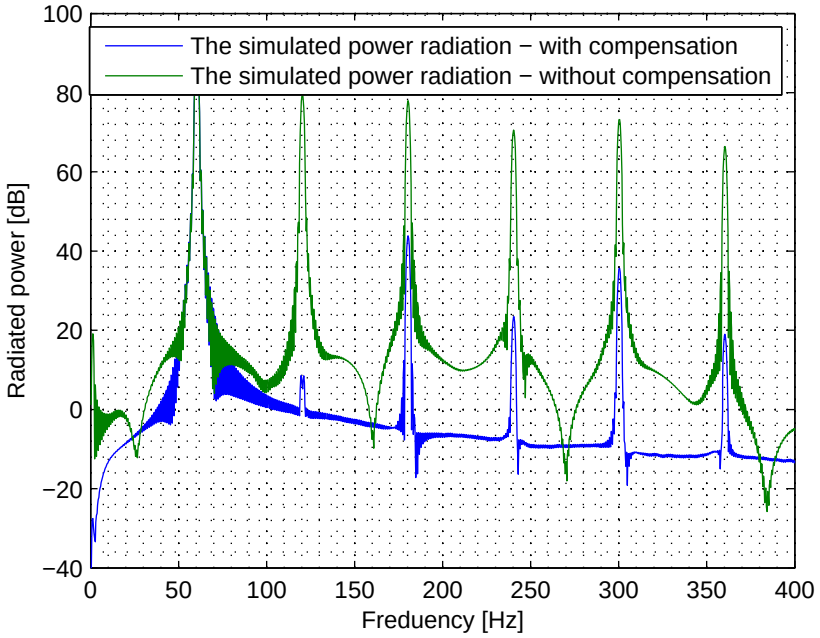

Figure 11.6: *Simulation of driver with state estimation and compensator in the nonlinear range.*

11.4 Summery

In this chapter the control scheme is tested on the driver. After the covariance noise was tuned a simulation was preformed in the linear range. A simulation in the nonlinear range produced an error, but analysing the problem showed a deviation in the settling time. By introducing a fix the simulation could be performed in the nonlinear range. The compensator did not remove the harmonic distortion, but did introduce a reduction. The third harmonic, which is the most dominating shown in 9.6 on page 57, was reduced with 36.85 dB in the linear range and 34.14 dB in the nonlinear.

Looking at the excursion of the nonlinear simulation, shown in Figure 11.5, clearly shows an improvement. The compensated excursion is more equally divided around zero, then the not compensated excursion.

The control scheme can reduce the harmonic distortion, but not remove it completely.

CHAPTER 12

Conclusion

In this thesis it was intended to prove the concept of removing the nonlinearities in a driver. The driver was described and analysed to create a mathematical model. The model was studied and due to the lower frequency range of a woofer driver, it was found that the eddy current was of no influence, and a state was removed from the model. The reduced model was compared with the initial model, and tests showed the reduced model was valid. Some measurements were done at Bang & Olufsen to compare the simulation with a real driver. This comparison showed that the model was valid.

The nonlinear parameters in the driver were inspected. These parameters were all dependent on the excursion. They where modeled as a fourth order polynomial. The coefficients to the polynomial were obtained using a Klippel Analyzer. The study of the parameters also showed that the temperature had an impact. This was not taken into consideration in this project, hence it was not considered to have influence on the harmonic distortion. To update the coefficients of interest three methods were presented, and one where preferable but none were implemented.

A nonlinear controller was designed to compensate for the nonlinearities. The scheme was a feedback linearization. The feedback linearization was chosen as the nonlinear controller due to its advantage of making a nonlinear system into a equivalent linear system. Afterwards the linear dynamic was applied, such that the nonlinearities were canceled out. This method showed to be sensible method, but the controller needed to be sampled with a sampling frequency larger than 44.1 kHz, which was not expected. The design of the controller also showed that full state information where needed, therefor a closed loop observer was designed.

The Extended Kalman filter was designed as the closed loop observer. The Extended Kalman filter estimated the remaining states of the nonlinear system. The observer was tested up against simulations of the driver, in the linear and nonlinear range, and found to be valid. The test showed that the observer is sensitive to noise - process and measurement. A test of the observer with the measurements made at Bang & Olufsen, where made. This test showed that the observer had some problems of estimate the states. It was concluded that the problem occurred due to the measurement device used.

The conclusion of the report, determines that it was not possible to remove the harmonic distortion, but possible to reduce them significant. The use of feedback linearization scheme used as controller is of advantage. But in order to obtain the benefit of the scheme, the observer used must have a good performance so that the estimation error of the states is very small.

12.1 Future Work

In order to get the controller system working, it is necessary to get real-time measurements in order to get the updated states and parameters. The drivers produced at B&O all ready have DSP implemented. A DSP can handle the necessary calculation needed. Implementing the controller on a DSP or similar devices, must be a step to verify the controller system in a driver setup. To accomplish this, some software generated in Matlab should be converted to software code, that can be executed on DSP.

Hence the change in performance of the driver, due to temperature change, age etc. the adaptive estimator block has to be implemented on the DSP such that the parameters can be identified. This can be done by use of the KF as described earlier, and seems a preferable method to use since the KF is implemented as closed loop observer.

The use of the EKF has shown to be a weel known method to observe the state in the driver, and can also be used to identify the parameters needed in the controller, either as an dual or joint estimator. As described the EKF has some drawbacks which can produce additional cost performance. In relation to the possible implementation on a DSP a method less computational can be used. A new novel method for calculating the states and parameters has been developed and could have been used. The method is known as the Uncented Kalman Filter (UKF). The method has been developed under the claim that it is easier to approximate a Gaussian distribution than it is to approximate an arbitrary nonlinear function or transformation. The UKF uses a deterministic sampling technique, the unscented transform to capture a set of samples (sigma points) around the mean. The nonlinear function is then applied to each point in turn to recover the true mean, and the covariance is also estimated by use of the covariance function. This type of filter provides a more accurate mean and covariance. The method requires less computation, hence the Jacobian is not the be calculated. The UKF can also be used to identify the parameters used in the controller.

Bibliography

Bright, A. Active control of loudspeakers: An incestigation of practical applications. Technical report, The Technical University of Denmark, Department of Accustic Technology - Ørsted - DTU, 2002. PhD Thesis.

Dickason, Vance. Loudspeaker Design. Audio Amateur Press, fifth edition, 1997. ISBN 1-882580-10-9.

Fitzgerald, Charles Jr., A. E.; Kingsley and Umans, Stephen D. Electric Machinery. Mc-Graw-Hill, Inc., 4th edition, 1983. ISBN 0-07-021145-0.

Grewal, Mohinder S. and Andrews, Angus P. Kalman Filtering - Theory and Practice Using MATLAB. Wiley-Interscience, second edition, 2001. ISBN 978-0-471-39254-5.

Hans Schurer, Cornelis H. Slump and Herrmann, Otto E. Theoretical and experimental comparison of three methods for compensation of electrodynamic transducer nonlinearity. J. Audio Eng. Soc., Vol. 46 no. 9, 1998.

Hedrick, J. K. and Girard, A. Control of Nonlinear Dynamic System: Theory and Applicatiions. Hedrick, 2005.

Khalil, Hassan K. Nonlinear Systems. Prentice Hall, 3th edition, 2002. ISBN 0-13-067389-7.

Klippel, Wolfgang. Loudspeaker nonlinearities causes, parameters, symptoms. J. Audio Eng. Soc, Vol. 46 no. 9, 1998.

Klippel, Wolfgang. Nonliear adaptive controller for loudspeakers using current sensor. In Audio Engineering Society. Audio Engineering Society, 1999.

Kreysig, Erwin. Advanced Engineering Mathematics. John Wiley & sons, inc., 8th edition, 1999. ISBN 0-471-33328-X.

Krump, G. Zur Temperaturabhängigkeit von Lautspecherparametern. DAGA, 1 edition, 1997. ISBN 3-9804568-2-X.

of Standards, National Institute and Technology. The hall effect, 2007. Visited 30/04-2008. URL `http://www.eeel.nist.gov/812/effe.htm`

Pedersen, Bo Rohde and Rubak, Per. Online identification of linear loudspeakers paramters. In Convention Paper 7060, 2007.

Technology, Audio. Flex units loudspeaker drivers, 2007. Visited 19/09-2007. URL http://www.flexunits.com/iz.asp?id=4%7Ca%7C119%7C%7C%7C

W. Marshall Leach, Jr. Introduction to Electroacoustics and Audio Amplifier Desgin. Kendall/Hunt Publishing Company, 2th edition, 1998. ISBN 0-7872-6093-2.

APPENDIX A

Eddy Current

The eddy current is a phenomenon that occurs when moving a conductor through a magnetic field, and where first discovered by the French physicist Lëon Foucault in 1851(Fitzgerald and Umans, 1983).

The eddy current is a current that is generated when a moving conductor experiences changes in the magnetic field generated by a static object, such as the magnet surrounding the voice coil. The eddy current is minimized by selecting magnetic core materials that have low electrical conductivity or by using thin sheets of magnetic material.

The eddy current build up inside the conductor due to the electrons experiencing a Lorentz force that is perpendicular to their motion.

The eddy current is the main reason for the skin effect in conductors carrying AC current. The skin effect is known as altering the AC current to distribute itself within the conductor. Thereby the density of the current is changed in a way where the density is higher at the surface than at the core.

The skin effect is where the resistance of the conductor changes as a function of frequency of the current. The resistance increases as the frequency is increased.

Klippel analysed the model, and proved that the use of a conductor in parallel with a resistance could decrease in influence of the eddy current.

APPENDIX B

State measurement

In order to test the simulation and estimation of the states, some measurement of states on a real driver would be useful. At B&O there where the facility to measure some of the states and define the input voltage for the driver.

Before being able to measure the states, a series of preparations and tests is necessary. The measurements are the voltage applied to the driver, the current measured in the driver, the acceleration of the diaphragm, and the velocity of the diaphragm. The signal processing is done in Matlab. For recording and sampling of data to and from the driver a standard MOTO 896HD (*sound-card*) is used. In addition for the setup extra hardware is needed.

The calibration of the sound-card and hardware is described in the following section, afterwards the result of the measurement of the states are presented.

The Matlab function `pa_wavplayrecord` is used to play and record sound from and to the sound-card.

B.1 Calibrating Sound-card and hardware

Mentioned earlier the signal processing in done by use of Matlab, and for that purpose different hardware is used, the sound-card and some additional hardware. The measurement setup is shown in figure B.1.

The calibrating of the hardware consists of different sub-test. The sub-tests are as follows.

1. Delay from input to output in the sound-card.
2. Amplification of the sensitivity, β, in the sound-card.
3. Gain in amplifier.
4. Excursion measurement by laser and determine gain.
5. Calibration of voltage measurement.
6. Calibration of accelerometer measurement.
7. Calibration of current measurement device.

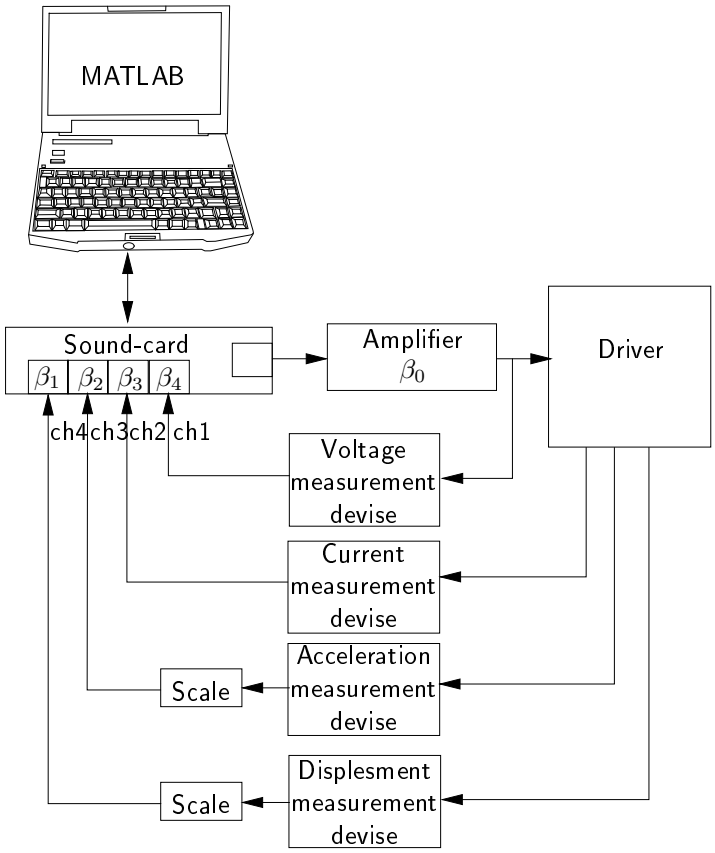

Figure B.1: *Hardware setup for measurements.*

B.1.1 Calibration of the sound-card

The sound-card is a standard sound device using a sampling frequency of 44.1 kHz and 24 bit converting, on 8 input, and 8 output channels.

For the test of the states, one output channel is used, and for recording the voltage, current, acceleration and velocity four is used channels on the sound-card.

The sound-card is calibrated by the two first sub-tests.

Between playing and recording a signal using the sound-card, there is a delay, which has to been known. By playing a known signal and recording the signal the delay in the sound-card can be determined the signal processing can be corrected according to the delay. The delay is measured to be 2164 samples using a sampling frequency of 44.1 kHz.

The sound-card used has an unknown internal sensitivity which needed to be known in order to use the correct values and units.

The determination of the internal sensitivity of the sound-card is done using a 1 kHz sinusoid signal, fed into the sound-card. The Root Mean Square (RMS) voltage applied to the sound-card is measured using a digital multimeter, and the recorded signal has a RMS value

$$b_{\mathrm{RMS}} = \sqrt{\frac{1}{N}\sum_{i=1}^{N} x_i^2}, \tag{B.1}$$

where x is the measured signal and N are samples recorded. The sensitivity of the sound-card is determined as

$$\beta = \frac{b_{\mathrm{RMS}}}{a_{\mathrm{RMS}}}. \tag{B.2}$$

Sound-card sensitivity

The internal sensitivity of the sound-card is ascertained as described early. Since the recording of the different signals are recorded on different channels on the sound-card the sensitivity for each channel used is to be determined.

The value of a_{RMS} is measured with a digital multimedia, showing a RMS value of 97.3 mV.

For the for channels used, different values of b are recorded and the RMS value of the recorded signal using (B.2) is calculated, and the result is shown in Table B.1

Table B.1: *Sensitivity of the channels used for recording signals.*

Channel	Gain	Gain [dB]
1	1.897	5.56
2	0.1361	-17.3212
3	0.1353	-17.377
4	0.1349	-17.398

B.1.2 Amplifier Gain

The sound-card has an output range of ± 1 V, and a amplifier is needed. The gain of the amplifier used, β_0 is calculated by the standard formula

$$G_{\mathrm{dB}} = 20 \log_{10} \left(\frac{v_1}{v_0} \right) \tag{B.3}$$

where v_1 is the voltage applied to the driver, v_0 is the voltage applied to the amplifier.

Using (B.3) the voltage applied to the driver can be determined. In professional power amplifier the gain is typical in the range of 20-40 dB. Choosing a input voltage to the power amplifier of 0.5 $\mathrm{V_{RMS}}$ and a gain of 26 dB results in a voltage applied to the driver at around 10 $\mathrm{V_{RMS}}$.

B.1.3 Excursion Calibration

The displacement of the diaphragm where measured using a laser. The laser hardware returns a voltage corresponding to the displacement measured in cm, meaning that measuring 1.3 V corresponds to 1.3 cm. Since the input on sound-card has a range of ± 1 V the signal needs scaling. The gain for the laser measurement is chosen to -6 dB.

B.1.4 Calibration of the Voltage

Since the amplifier has a 26 dB gain, the voltage applied for the driver is in the range of 10 V. To be able of record the voltage the signal needs to be scaled. For the scaling an amplifier with a gain of -40 dB is used.

B.1.5 Calibration of the Accelerometer

The acceleration of the diaphragm is measured by use of a standard accelerometer, which is mounted on the diaphragm, and the voltage corresponding to the acceleration, is measured in m/s and returned in mV. The signal does not move outside the range of the sound-card, therefor no scaling is needed.

B.1.6 Calibration of the Current

The current applied to the driver is measured using a current measuring device. This device measures the magnetic flux generated inside a voice coil. This measurement of the current is outputted in volt scaled by a factor 10.

B.2 Measurements Result

The obtained calibration values are used in a Matlab script to calculate the correct values recorded.

The input signal used is a 10 V_{RMS} at 60 Hz. The measured states are show in Figure B.2.

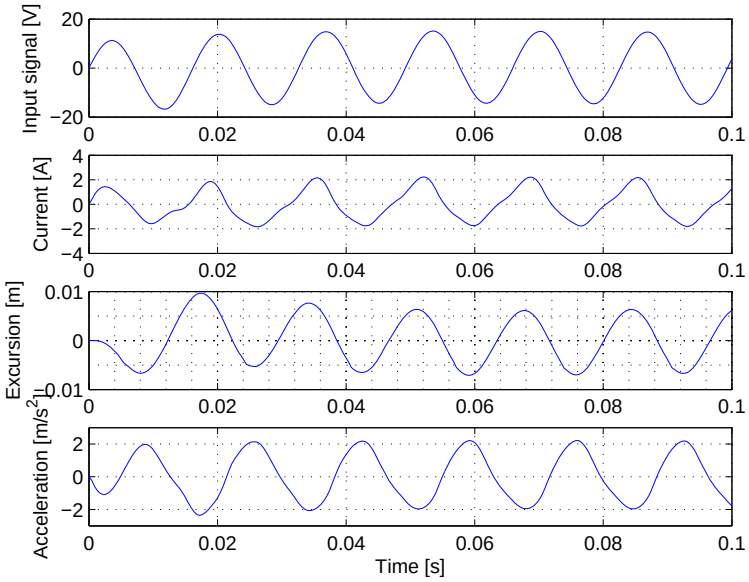

Figure B.2: *The measured states of a 60 Hz signal.*

The results shown is almost as expected. The input voltage is almost at the chosen value. There is a difference of approximately 0.4 V between the desired 10 V_{RMS} and the measured. The difference is acceptable and the gain is considered correct. The current measurement does not look like a pure sinusoid. Around zero the measurement has a deviation which is not expected. The movement of the excursion does not have any deviation, and thereby the movement of the voice coil must be expected without deviation. The error must therefor be in the measurement device. The current measurement is analysed with a FFT. The measurement only consist of the 60 Hz signal the harmonics. The excursion measurement starts with a small deviation, but quickly settle around zero. The measurement is correct compared with the Klippel analyser. The acceleration measurement is made without having data to compare it with. But the movement of the excursion gives an idea of the acceleration.

B.3 Summery

The sound-card has been calibrated and a measurement of the states has been preformed. The data is acceptable but the current measurement has a deviation. This deviation is considered small and the data can be used in a simulation with real data.

APPENDIX C

Klippel Analyzer

The Klippel Analyzer is a tool for analysing drivers. The analyser determines numerous parameters through testing.

C.1 General

The Klippel Analyzer consists of the Klippel R&D system. This system is a tool for development, manufacturing and quality control of drivers developed by Wolfgang Klippel. The system consists of a distortion analyzer, a laser and an amplifier. The system uses the laser aimed at the diaphragm to measure the excursion, the current in the driver is also measured. These two states are used as inputs to the distortion analyzer. From the distortions analyzer, a known audio signal is outputted and applied to the driver through the amplifier. The test runs for several hours which insures the longterm parameters have changed. The test can be executed on the analyzer or via a PC running dB-Lab software.

The distortion analyzer works by using system identification. The analyzer performs two tests, one for the linear and one for the nonlinear parameters. The first test needs information about the driver as diameter and weight. Using the current and excurstion as inputs, the linear parameters are identified. The second test determines the nonlinear parameters. The test uses the linear parameters. Since the nonlinear parameters are not directly measurable, the analyzer adapts a nonlinear model of a driver. From the measured current and excursion and audio signal, the nonlinear model is adapted so it fits the test speaker. When the model is adapted to the test driver, meaning the outputs are identical, the nonlinear parameters are approximated.

C.2 Measurements

B&O in Struer provided a Distortion Analyzer 2 (DA2) for this project. The DA2 can through test determine the linear and nonlinear parameters of the driver. B&O has preformed and provided the parameters for the driver used in this project.

For confirmation purpose a test is preformed which measures the second state, the excursion of the diaphragm. The DA2 is used in combination with the laser, providing the excursion of the diaphragm in cm.

The measurement test can be seen in appendix B on page 77.

APPENDIX D

Modelling the parameters

The parameters used in the thesis are modelled by using a Matlab script. In section 3.3 the linear parameters are described, and these are used directly. The nonlinear parameters, are modelled as a fourth order polynomial where the coefficients are provided from the Klippel Analyzer.

The script uses the `polyval` command to evaluate the coefficients from the given excursion. The `polyval` command takes the five coefficients and excursion as input and returns the value of the polynomial.